Masterthesis: QCD Analysis of the Proton Structure Function with Unintegrated Parton Densities

Van Spilbeeck Alex

November 15, 2011

Contents

1 Introduction **2**
1.1 Kinematics and notations . . . 2
1.2 The Standard Model . . . 2
1.2.1 Composite particles . . . 4
1.3 DIS . . . 5
1.3.1 Structure functions and parton density functions . . . 5
1.3.2 Higher order interactions and gluon density functions . . 7
1.3.3 Scaling violation and Q^2 dependence . . . 7
1.3.4 Renormalized distributions . . . 10
1.3.5 `DGLAP` equations . . . 11
1.4 Splitting functions . . . 11
1.5 Coupling α_s . . . 12
1.6 What is an unintegrated parton density? . . . 13
1.6.1 The effects of transverse momentum . . . 13

2 Unintegrated parton density functions **16**
2.1 `Pythia8` . . . 16
2.1.1 Kinematics . . . 17
2.1.2 Z-boson . . . 18
2.1.3 Higgs boson . . . 19
2.2 Kimber, Martin and Ryskin method . . . 19
2.2.1 `KMR` Integrals . . . 19
2.2.2 Parton density functions and `LHAPDF` . . . 20
2.2.3 Integration of the pdf . . . 21
2.2.4 The T_q-factor . . . 21
2.2.5 The T_g-factor . . . 21
2.3 `CCFM` unintegrated gluon density function . . . 23
2.4 Results . . . 24
2.4.1 Gluon density functions . . . 24
2.4.2 Quark density functions . . . 24

3 Evolution of gluon density functions **31**
3.1 Evolution of the gluon density function 31
3.2 Evolution of the distribution 32
3.2.1 Fixed α_s 33
3.2.2 Non-fixed α_s: $Q = q_t$ 36
3.3 Results 38
3.3.1 Integrated parton densities 38
3.3.2 Unintegrated parton densities 38
3.4 Calculation of F_2 40
3.4.1 k_T independent calculation 44
3.4.2 k_T dependent calculation 44
3.4.3 F_2 results 46

4 Goals and Conclusions **49**

A Subatomic particles and dynamics **50**
A.1 Four-momentum and the mass shell 50
A.2 Virtual particles 50
A.3 Mandelstam variables 51

B Extraction of 4D convolution in `Pythia8` **52**
B.1 Names 52
B.2 Evolution in `Pythia8` 52
B.3 The algorithm 53

C Monte Carlo techniques and integration **55**
C.1 Non-uniform distributions 55
C.2 Monte Carlo integration 56

D Structure function F_2 results **58**
D.1 $\Lambda = 200$ MeV 58
D.2 $\Lambda = 250$ MeV 62
D.3 $\Lambda = 300$ MeV 66

E Logarithmic bins **70**

1 Introduction

1.1 Kinematics and notations

In particle physics one of the most important principles is the equality of matter and energy via Einstein's

$$E = mc^2. \tag{1}$$

This leads to the introduction of a new physical quantity, the four-momentum of a particle. Properties of four-momentum are not discussed here but can be found in the appendix A.

Because of this transition between matter and energy a lot of factors c would have to be written in the equations where mass, momentum and energy are treated equally. To avoid a cumbersome notation with lots of constants we use

$$c = \hbar = \varepsilon_0 = 1. \tag{2}$$

c is the speed of light, $\hbar$ is Planck's constant and ε_0 is the permittivity of the vacuum. This allows us to treat energies, momenta and masses the same way. However, at the end of the ride we do need these values to obtain the proper values of the results. The constant c can then be entered were needed by running a dimensional analysis over the result.

So, were a mass m, a momentum p and an energy E are summed over, we in fact mean mc^2, pc and E.

All three adjusted constants also appear in the value of the coupling strength α of the electromagnetic interaction, otherwise known as the fine-structure constant:

$$\alpha = \frac{e^2}{4\pi\varepsilon_0\hbar c} = \frac{e^2}{4\pi} \approx \frac{1}{137}. \tag{3}$$

$-e$ is the electrical charge of the electron.

1.2 The Standard Model

The Standard Model of particle physics is the theory describing all known elementary particles and three of the four interactions between them (the strong, electromagnetic and weak interaction). These particles are divided into two groups:

- **Fermions**: These are elementary particles with a non-integer spin value. Fermions can be divided into two groups.
  - **Quarks**: There are six different types of quark flavours: *up*, *down*, *charm*, *strange*, *top* and *bottom*. The up and down quark are most common and combine to form neutrons and protons, the building blocks of atoms and the matter in the universe. Quarks have an electric charge (either $+2/3$ or $-1/3$) as well as a colour charge (*red*, *green* or *blue*). This makes that they are the only fermions that do feel the strong interaction and are always *confined* within a composite particle: a quark can not exist as an isolated particle. The only (known) colour combinations that can exist isolated are called *white*: red-green-blue (three quarks in a hadron) or colour-anticolour (a quark and an antiquark in a meson).

– **Leptons**: There are three couples of leptons, each consisting of a charged lepton and its neutrino counterpart. These charged leptons are called: *electron* (e), *muon* (μ) and *tau* (τ), and their neutrinopartners are called *electron neutrino* (ν_e), *muon neutrino* (ν_e) and *tau neutrino* (ν_e). The charged leptons carry an electrical charge $Q = -1$, the neutrinos carry no electric charge and are nearly massless, so they can only interact via the weak interaction. While the mass of the neutrino is not known, it is known that they are massive. Neutrino's are subject to an effect called "oscillation"[1] , which is only possible if the neutrino's are massive.

These particles can also be divided into three generations: each generation contains an electron type particle, a neutrino, an up and a down type quark. All fermions also have an antiparticle: a particle with exactly the same properties (mass, spin, etc.) but with an opposite electrical charge. The following table shows the fundamental fermions of the Standard Model, with each row corresponding to a generation. In the brackets the mass and the uncertainty thereof are given [2].

Fermions			
Leptons		Quarks	
$Q = -1$	$Q = 0$	$Q = +\frac{2}{3}$	$Q = -\frac{1}{3}$
e (0.51 MeV)	ν_e (< 2 eV)	u (1.7-3.1 MeV)	d (4.1 - 5.7 MeV)
μ (105.7 MeV)	ν_μ (< 2 eV)	c ($1.29^{+0.05}_{-0.11}$ GeV)	s (100^{+30}_{-20} MeV)
τ (1.78 GeV)	ν_τ (< 2 eV)	t ($172.9 \pm 0.6 \pm 0.9$ GeV)	b ($4.19^{+0.18}_{-0.06}$ GeV)

- **Bosons**: Particles with an integer spin and responsible for the three elementary forces in the Standard Model.

  – **Gluons (g)**: The bosons responsible for the strong force which binds the nucleons in atomic nuclei, and quarks in these nucleons. Gluons carry a colour-anticolour charge and so exist in eight different charges, as the ninth possible state is white and thus insensitive to the strong force. Since gluons themselves carry colour-anticolour charge they are sensitive to the strong force and can interact with one another. Gluons are massless particles. The branch of particle physics dedicated to the strong interaction is called Quantum Chromo Dynamics (QCD).

  – **Photons (γ)**: The massless and chargeless carrier of the electromagnetic interaction. It can only interact with particles that carry electric charge, but it can travel over very large distances due to its masslessness. The photon is the only fundamental boson whose effects can be felt at larger scales (for example the light of the sun and distant stars).

[1] Neutrino oscillation is an effect in which the type of a neutrino will change. This effect is the reason why there are not only electron neutrino's radiated by the Sun's fusion process: on their way to Earth, some electron neutrino's oscillate to a different type.

– Z^0, $W^\pm$ **bosons**: These particles are the carriers of the weak interaction. They are massive particles with masses of about 80 GeV ($W^\pm$) and 91 GeV (Z^0). Via electroweak unification, the weak bosons are very closely linked with the photon.

– **Higgs boson (H^0)**: The famous Higgs mechanism and Higgs boson (H) are needed to explain the mass of the massive gauge bosons of the weak interaction. The photon and the weak bosons can be treated as superpositions of four electroweak bosons, and this can be seen in the electroweak Lagrangian. However, this Lagrangian does not assign any mass to the weak bosons, while they are known to have mass. This problem can be solved by the Brout-Englert-Higgs mechanism, which creates the mass of the weak gauge bosons. When the BEH mechanism is treated as a part of the Standard Model theory, a new particle emerges: the Higgs boson. The Higgs boson has not yet been discovered, but it is already known that if it exists, it would have to be heavier than 115 GeV. It has not been seen at lower energies, and thus can not exist (as theory predicts it) below this mass threshold. The Higgs can only interact with particles that have mass.

  Please note that there are several theories surrounding the Higgs boson, some introducing as much as five new Higgs bosons. None of these theories has been confirmed by discovery, but where the Higgs appears in this thesis, it is assumed only one chargeless version exists.

The following table shows the gauge bosons of the Standard Model theory, their masses [2] and their corresponding interactions. The Higgs has been added, but note that this still is an unconfirmed hypothesis.

Bosons				
Strong interaction	Electroweak unification			
	Electro-magnetism	Weak interaction		Gauge boson mass
$Q = 0$	$Q = 0$	$Q = 0$	$Q = \pm 1$	$Q = 0$
g (0)	γ (0)	Z^0 (91.1876 GeV $\pm$ 0.0021 GeV)	$W^\pm$ (80.399 GeV $\pm$ 0.023 GeV)	H^0 (> 114.4 GeV)

1.2.1 Composite particles

Fermions and bosons combine to form more complex particles, like the well known proton. This is not a fundamental particle but is essential to this thesis. The proton contains three *valence quarks*: two up quarks and one down quark. As we will see later, this is just the "net content" of the proton. The quarks within this composite proton are bound together by the strong force and its gluon messengers.

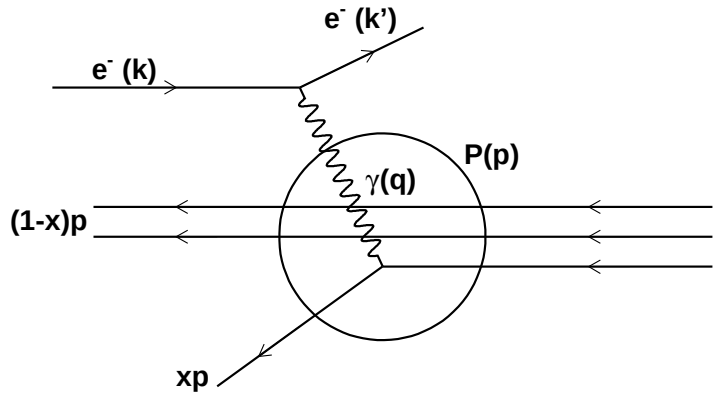

Figure 1: Schematic representation of DIS: an electron (initial four-momentum k) exchanges a photon (four-momentum $q = k' - k$) with a quark in the proton and breaks the proton up. The fragments of the proton are a quark that carries a fraction x of the proton's total four-momentum p, and a diquark state carrying the rest of the proton's four-momentum.

1.3 DIS

1.3.1 Structure functions and parton density functions

Parton density functions [1] are an essential part of the QCD theory. Electrons are fundamental and pointlike particles (as far as we know) and in collisions all their four-momentum will be completely transferred to the particles in the final state. Protons are not fundamental but composed of quarks and gluons (collectively called partons). To investigate the constituents of the protons we may use deep inelastic scattering (DIS) of electrons on protons.

An schematic representation of DIS is shown in figure 1. An electron with four-momentum k approaches a proton and interacts with the quarks in the proton by exchanging a photon. The photon carries a four-momentum of $q = k - k'$ and is offshell (its mass is not zero). The proton carries a four-momentum p, which is divided between the quarks. If the four-momentum carried by the photon is high enough, the proton may break up in different parts with four-momentum fractions x and $1 - x$. We can speak of DIS if the total sum $W^2 = (p + k)^2$ and the exchanged four-momentum $Q^2 = -q^2$ are both very high (compared to the mass of the proton).

The big challenge with DIS is to get a cross section[2] σ that takes into account

[2]The cross section is a rate with which certain types of happen, or how often a certain final state appears. The cross section is expressed in the non SI unit *barn*, a measure for area. A differential cross section is a measure of probability that takes a certain dependence into account, e.g. the energy of the collision.

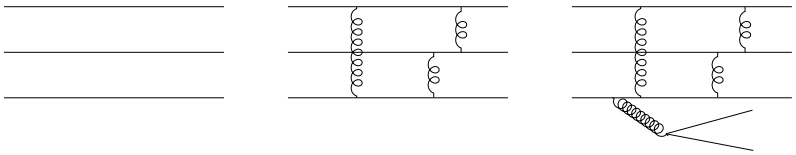

(a) (b) (c)

Figure 2: Three different ways to look at the proton: only valence quarks; valence quarks and gluons; valence quarks, gluons and sea quarks.

the complexity of the proton. Such a cross section can be calculated with the help of the so-called structure functions F_1 and F_2:

$$\frac{d^2\sigma}{dxdQ^2} = \frac{4\pi\alpha^2}{Q^4}\left[(1+(1-y)^2)F_1 + \frac{1-y}{x}(F_2 - 2xF_1)\right] \tag{4}$$

where x (¨Björken x¨) is the energy-momentum fraction carried by the quark and the inelasticity y is a measure for the angle of the outgoing particle. The explicit expressions for these two variables are:

$$x = \frac{Q^2}{2p\cdot q} \tag{5}$$

$$y = \frac{q\cdot p}{k\cdot p} \tag{6}$$

The structure functions are a way to express our (lack of) knowledge of the proton's contents. The expression of F_2 is

$$F_2 = x\sum_q e_q^2 q(x) \tag{7}$$

where q sums over all quark- and antiquark flavours, e_q is the charge of each quark flavour and $q(x)$ is the quark density function per flavour. The quark density functions represent the quarkcontent of the proton for each (anti)quark flavour and for each value of x. Experiments have shown that there are particles present in the proton that are not predicted by the classical image of the proton.

Let's take a look at figure 2: these three diagrams show the evolution of the quark parton model.

Figure 2a shows a proton as a combination of three valence quarks that do not interact with each other. In this scenario the quarks have a fixed x value: $x = \frac{1}{3}$. Two up quarks and a down quark can be found in the proton, and every quark carries a different of three colour charges: red, green or blue.

Figure 2b shows a proton where the valence quarks can interact with each other via the exchange of gluons. This causes their x values to change as the quarks exchange energy and momentum. x will be smeared out around $\frac{1}{3}$. The quarks will always be two up quarks and one down quark, as the flavour of the quarks cannot change. The colourcharge of the quarks changes, but the total colourcharge (quarks and gluons together) will be white.

Figure 2c shows a proton where the valence quarks can interact with each other and emit gluons that will split into a quark-antiquark pair. This dramatically changes the structure of the proton: there will be many partons with low x value. The collection of quarks and antiquarks that originate from gluonsplitting are called seaquarks. Since a gluon interacts with all six quark flavours it is possible to find heavier flavours (c, s, b) in a proton[3]. The colour charge of the partons will change because of the gluons, but the overall charge will be white.

All seaquarks cancel against one another: for every seaquark, there is a sea antiquark of the same flavour. So the valence quarks are the net quark content of the proton, but not the total content.

Experiments have shown that about 50% of a proton's energy and momentum is carried by gluons and about 13% is carried by antiparticles, leaving 37% for the quarks[4] [3].

1.3.2 Higher order interactions and gluon density functions

The gluon density function $g(x, Q^2)$ can not be directly measured by simple photon scattering: the gluon carries no electric charge and the photon carries no colour charge, making interaction between the two not possible if we only work with first order Feynmandiagrams. However, it is possible to measure the gluon density function in higher order diagrams . There is a process[5] in $\mathcal{O}(\alpha_s^1)$ which depends on the gluon content of the proton: boson-gluon fusion (BGF). Here, the incoming photon interacts with the gluon via the exchange of a virtual quark, which results in the creation of quark-antiquark pair.

If the BGF process is included in the calculation of the cross section, the gluon density functions will also appear. Thus it is possible to measure the gluon density even though direct interaction between gluon and photon is impossible.

Another higher order interactions is the QCD Compton process. In this interaction a photon interacts with a quark before or after emission of a gluon. This process can not be used to measure proton's gluon contents, but will be needed to calculate higher order interactions correctly.

1.3.3 Scaling violation and Q^2 dependence

Experiments have shown that the structure function F_2 is scale dependant. This is than interpreted as a scale dependence of the parton density functions[6] $a(x)$. A photon interacting with the proton can resolve its transverse details, like the transverse momenta of the partons. What the photon will see is the projection of the proton on the transverse plane (the $x - y$ plane, with z the axis of the proton movement). If λ is the photon's wavelength and ϑ the scattering angle

[3]Note that the top has been left out: with its weight of 172 GeV it is very unlikely to exist within a 1 GeV proton. And since the seaquarks are created in particle-antiparticle pairs there would be two tops, resulting in a whopping 344 GeV. As a result the top is not present in `Pythia8`'s simulated collisions.

[4]The contribution of antiquarks is very low because they can only be found in the low energetic particles of the sea. The contribution of the quarks is much higher because it encompasses both seaquarks and valence quarks, the latter still carrying a significant fraction of the proton's momentum.

[5]Processes with one strong interaction vertex.

[6]Note that this can be either a quark density function $q(x)$ or a gluon density function $g(x)$

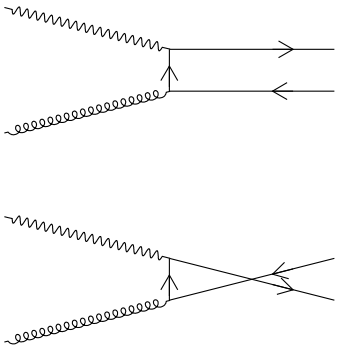

Figure 3: Boson gluon fusion (BGF), a higher order interaction between a photon and a gluon. The BGF process can be used to determine the gluon density function of the proton.

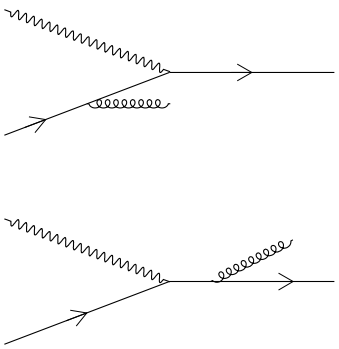

Figure 4: QCDC, a higher order interaction between a photon and a quark.

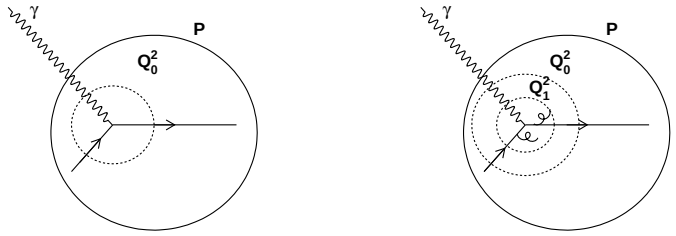

(a) Q_0^2 (b) Q_1^2

Figure 5: Comparison of two photons with different energy: $Q_0^2 < Q_1^2$. The more energetic photon has a shorter wavelength and can resolve more details. The second photon is able to see the two gluons radiated by the quark while the first photon can not.

between the photon and the z-axis, then the resolution of transverse details will be

$$\frac{\lambda}{\sin\left(\frac{\vartheta}{2}\right)} = \frac{h}{p}\frac{1}{\sin\left(\frac{\vartheta}{2}\right)} \tag{8}$$

$$= \frac{2h}{q} \tag{9}$$

where $\lambda = \frac{h}{p}$ with p the photon's momentum, h Planck's constant and q the momentum exchange. A higher photon momentum p will return a higher exchanged momentum q (and thus higher Q^2) and lead to a better resolution of the proton's structure.

This is illustrated in figure 5: two photons of different energy scatter on a quark inside the proton. The low energy photon (Q_0^2) has a longer wavelength and will not be able to see the smaller details of the proton. The high energy proton (Q_1^2) has a shorter wavelength and will be able to resolve many details at a smaller scale. Examples of these details are low energetic gluons that radiate of the quark before and after it interacts with the photon. It can be said that a photon will see more particles if that photon has a high enough energy scale Q^2.

This Q^2 dependence means that the parton density function also will depend on the scale at which the proton is probed: $a(x, Q^2)$. A parton density function can also be evolved from a lower to a higher scale: if we know what the density function looks like at scale Q_a^2, do we know what it looks like at the higher scale Q_b^2? This evolution means that $a(x, Q^2)$ changes with increasing Q^2. We interpret this as following: at a scale q^2 the resolution of the photon is high enough to see that a parton a "splits" into two new particles. What looked like a single particle at lower scales are in fact two particles with lower energy that can be detected as such at higher scales.

1.3.4 Renormalized distributions

The introduction of higher order contributions also means a change in cross section for DIS. The differential cross sections for BGF and QCDC are of the forms

$$\frac{d\sigma^{BGF}}{dk_T^2} = \sigma_0 e_q^2 \frac{\alpha_s}{2\pi} \frac{1}{k_T^2} \left[P_{qg}(z) + ...\right] \quad (10)$$

$$\frac{d\sigma^{QCDC}}{dk_T^2} = \sigma_0 e_q^2 \frac{\alpha_s}{2\pi} \frac{1}{k_T^2} \left[P_{qq}(z) + ...\right]. \quad (11)$$

The scale k_T^2 is the transverse momentum of the gluon, and the splitting functions $P_{qq}(z)$ and $P_{qg}(z)$ represent the possibility that a parton (q or g) emits another quark that carries a fraction z of the original parton's energy-momentum. Expressions for the splitting functions are given in section 1.4.

After integration over the transverse momentum the cross sections will contain a logarithm $\ln\left(\frac{Q^2}{\chi^2}\right)$, where the scale χ^2 is an arbitrary lower cut-off introduced to prevent divergence in the cross section. This cut-off is arbitrary but may not influence the results: the effects of scales below χ^2 will be absorbed into the bare quark distribution q_0 (see below).

The higher order contributions also change the structure function F_2:

$$F_2 = x \sum e_q^2 \left[q_0(x) + \int \frac{dx_2}{x_2} q_0(x) \frac{\alpha_s}{2\pi} P_{qq}\left(\frac{x}{x_2}\right) \ln\left(\frac{Q^2}{\chi^2}\right) + C_q(z) + ...\right]. \quad (12)$$

The integral represents a single quark radiated of another quark, taking with it an energy-momentum fraction of x of the initial partons fraction x_2. Of course, seaquarks can also be radiated by gluons[7]: this is represented in a very similar integral over $P_{qg}(z)g_0(z)$ (following after +...).

The distributions $q_0(x)$ are called bare distributions and would be the correct pdf's if there were no higher order contributions. These bare distributions can not be measured: if we increase the scale of our probing photon we will just see more and more partons radiate of our original parton. We need to define what we see as the parton, and what we see as radiation of the parton. To illustate this we look at figure 5. We can choose to take Q_1^2 as the lower scale: anything below this scale is "part of the quark". This would mean that the two radiated gluons are components of the quark and should not be seen as individual particles. This lower cut-off scale is called $\mu^2 (\gg \chi^2)$ and is completely arbitrary. Any divergent effects can be absorbed in the bare quark density function $q_0(x)$.

The introduction of μ is called renormalization and will change our pdf's. The pdf will now be

$$q(x,\mu^2) = q_0(x) + \frac{\alpha_s}{2\pi} \int_x^1 \frac{d\xi}{\xi} \left[q_0(\xi) P_{qq}\left(\frac{x}{\xi}\right) \ln\left(\frac{\mu^2}{\chi^2}\right) + C_q\left(\frac{x}{\xi}\right)\right] + ... \quad (13)$$

This new distribution is now the bare distribution plus all emissions by the parton between our antidivergence cut-off χ and our newly introduced cut-off μ. The variable ξ is the energy-momentum fraction (with respect to the

[7] This "radiation" is the splitting of a gluon into a quark-antiquark pair.

proton) carried by the emitting particle, x is the energy-momentum fraction (with respect to the proton) and these two are related via z:

$$x = z\xi. \tag{14}$$

We still see the arbitrary cut-off scale χ^2 in the expression but it will not influence $q(x, \mu^2)$. If χ^2 changes in the integral the bare distribution q_0 will be adjusted to compensate for this.

Gluon density functions are renormalized in an analogous way.

1.3.5 DGLAP equations

The cut-off χ^2 has been taken care of, but the issue of the other arbitrary scale μ^2 still remains. To get rid of this dependency the structure function F_2 is calculated:

$$F_2(x, Q^2) = x \sum e_q^2 \int \frac{d\xi}{\xi} q(\xi, \mu^2) \left[\delta\left(1 - \frac{x}{\xi}\right) + \frac{\alpha_s}{2\pi} P\left(\frac{x}{\xi}\right) \ln\left(\frac{Q^2}{\mu^2}\right) \right]. \tag{15}$$

F_2 cannot depend on the scale μ^2 but in its current form the structure function is influenced by μ^2. To solve this problem we need to demand that there is no cut-off dependence:

$$\frac{\partial F_2}{\partial \mu^2} = 0. \tag{16}$$

From this condition one can derive the so-called DGLAP (Dokshitzer-Gribov-Lipatov-Altarelli-Parisi) equations:

$$\frac{dq_i(x, \mu^2)}{d \ln \mu^2} = \frac{\alpha_s}{2\pi} \int_x^1 \frac{d\xi}{\xi} \left[q_i(\xi, \mu^2) P_{qq}\left(\frac{x}{\xi}\right) + g(\xi, \mu^2) P_{qg}\left(\frac{x}{\xi}\right) \right] \tag{17}$$

$$\frac{dg(x, \mu^2)}{d \ln \mu^2} = \frac{\alpha_s}{2\pi} \int_x^1 \frac{d\xi}{\xi} \left[\sum_i q_i(\xi, \mu^2) P_{gq}\left(\frac{x}{\xi}\right) + g(\xi, \mu^2) P_{gg}\left(\frac{x}{\xi}\right) \right] \tag{18}$$

$$\tag{19}$$

where the index i has been added to the quark density functions to indicate the different quark flavours.

This set of equation provides a way to calculate parton density functions without the arbitrary μ^2 influencing the result.

1.4 Splitting functions

The splitting functions are a measure for the splitting probability: if we have a parton a, what is the probability it will split at any scale μ^2 into two particles? These functions are written as $P_{ab}(z)$: the probability that particle b will emit a particle a that carries a fraction z of b's energy-momentum fraction.

The splitting functions P_{gq} and P_{qq} do not represent an actual splitting of the quark but the emission of a gluon with momentum fraction z and $1 - z$. The original quark will continue to exist but with a different colourcharge. P_{gg} represents a gluon which splits into two new gluons: the two gluons have two different colour-anticolour charges and none of these is the same as that of the

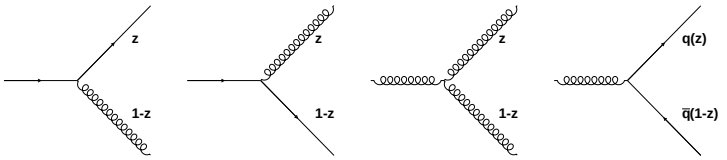

(a) P_{qq} (b) P_{gq} (c) P_{gg} (d) P_{qg}

Figure 6: The four different splitting functions.

original gluon. The last splitting function represents the decay of a gluon into a quark-antiquark pair of the same flavour.

The expressions of the different splitting functions are:

$$P_{qq}(z) = \frac{4}{3}\left(\frac{1+z^2}{1-z}\right) \tag{20}$$

$$P_{gq}(z) = \frac{4}{3}\left(\frac{1+(1-z)^2}{z}\right) \tag{21}$$

$$P_{gg}(z) = 6\left(\frac{1-z}{z} + \frac{z}{1-z} + z(1-z)\right) \tag{22}$$

$$P_{qg}(z) = \frac{1}{2}\left(z^2 + (1-z)^2\right) \tag{23}$$

We can derive from these splitting functions that at low x the proton will be dominated by the gluons. Low x partons can be created via low z splitting. For a low value of z the function $p_{gg}(z)$ will have the highest value: gluons are most likely to split into low z gluons, which in turn can again emit low z gluons. This is the reason that for some calculations done later in this thesis only use gluons as a proton's content.

1.5 Coupling α_s

Any interaction involving gluons is governed by the strong interaction. For any vertex with a gluon in Feynmandiagram, the strong coupling α_s appears in the associated calculations. As is also the case with the electromagnetic interaction and its coupling α, the strong coupling is in fact not a fixed constant but a variable, determined by the scale of the interaction. The main difference between the strong interaction and the electromagnetic interaction is the fact that the electromagnetic interaction gets stronger at high energies/short distances, while the strong interaction gets weaker at high energies/lower distances. This due to effects which are called screening (EM interaction) and anti-screening (strong interaction).

The analytical expression of α_s can be calculated via perturbation theory. The expression used in this thesis is

$$\alpha_s\left(Q^2\right) = \frac{12\pi}{(33-2n_f)\ln\left(\frac{Q^2}{\Lambda^2}\right)}. \tag{24}$$

Q^2 is the scale at which we wish to know the strength of the interaction. Please note that this may be the exchanged four-momentum squared of the interaction (as introduced in section 1.3.1), but other scales are possible as well. n_f is the number of quark flavours that can appear: whether a quark can be created or not depends on the energy available in the process: if the scale of a process is too low, it is not likely that heavy quark like the top quark or the bottom quark will appear. Λ (or Λ_{QCD}) is an integration constant which appears when solving the renormalization equation for α_s. This is the one fundamental constant in QCD which has to be fixed by experiment. For simplicity these parameters were chosen fixed at $n_f = 4$ or 5, depending on the exact scale Q^2, and $\Lambda = 250$ GeV unless another value is mentioned.

1.6 What is an unintegrated parton density?

The integrated parton density function depends only on the values of x and Q^2: the function says how many partons with four-momentum fraction x we can observe at a probing scale Q^2. These functions are frequently used in calculations, but do not always reflect the proton's content correctly. An integrated parton density function does not use the parton's transverse momentum k_T, which may lead to false kinematic results, see the section about initial state radiation.

To avoid these incorrect results one may opt to use unintegrated parton densities $a(x, k_T^2, Q^2)$ (updf's), where the transverse momentum of the parton is explicitly mentioned. The integrated parton density function can be calculated from the updf via integration over all values of k_T:

$$a(x, Q^2) = \int dk_T^2 \; a(x, k_T^2, Q^2) \tag{25}$$

where we need to remember that the transverse momentum is a vector in the twodimensional (x, y) plane perpendicular to the z-axis. An integrated parton density $a(x, Q^2)$ is automatically assumed to be the integral over all possible unintegrated parton density values for values (x, k_T^2).

An example of the importance of the unintegrated parton density function is illustrated by the initial state radiation.

1.6.1 The effects of transverse momentum

If a proton moves along an axis z with no transverse momentum at all, then the partons within the proton are likely not to have a high transverse momentum k_T. The partons can have a value for k_T as long as the total partonic transverse momentum equals the zero value of the proton's transverse momentum. However, it is possible for two protons along a single axis to collide and create particles with high transverse momentum. This is due to initial state radiation (ISR).

A parton originating from one of the two protons can be the subject of many parton splittings and emissions. At each splitting a new particle will come into existence, and this particle will carry non-zero momentum. Due to conservation of momentum the initial parton will change its own transverse momentum, which may lead to an increase of k_T. It is possible that the parton will experience many splittings and emissions, and thus it can develop a significant transverse

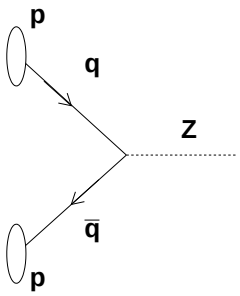

Figure 7: The lowest order diagram for $q\bar{q} \to Z$. A quark and an antiquark of the same colour annihilate and create a Z boson.

momentum. Two high k_T partons interacting in a two-to-one collision may create a particle with very high transverse momentum[8] p_T.

An example of this effect is the creation of a high p_T Z boson from a quark and an antiquark (figure 9a). A simulation is shown in figure 8: a number of $q\bar{q} \to Z^0$ collisions are simulated, N times with ISR and N times without ISR. Several values of $\sqrt{s}$, the energy of the collision, are used. Without ISR (dashed lines) the partons are not able to build up a high transverse momentum and the p_T distribution of the resulting Z^0 will be very narrow and peaked. If ISR is allowed (full lines) the partons can gather a high k_T value and transfer it to the created boson: this results in a high tail for the p_T distributions. We can also see that at higher $\sqrt{s}$ values the tail of the distribution will be longer. From experiments we know that high p_T values occur and thus the transverse momentum and the evolution thereof should be included in calculations.

The calculation of the unintegrated parton density function is the subject of the next section.

[8]May, because the transverse momentum is a twodimensional vector quantity in the $x - y$ plane. If the momenta of the colliding particles are of opposite direction, the resulting particle ends up with a low p_T.

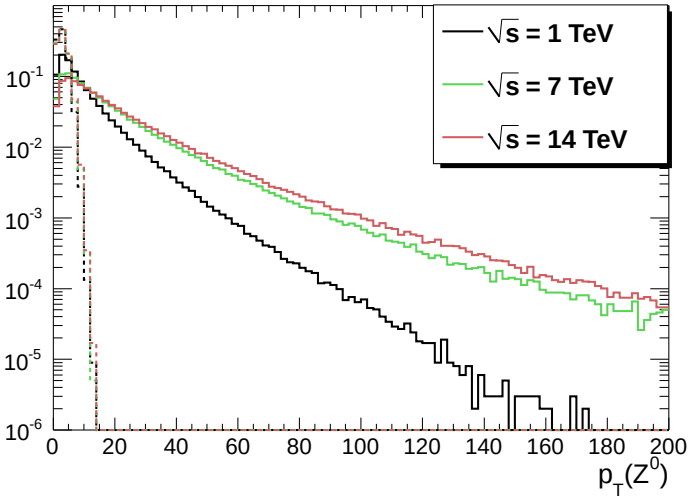

Figure 8: Simulation of the $q\bar{q} \rightarrow Z^0$ process at different energies, with and without ISR. $\sqrt{s}$ is the energy of the colliding protons. The full lines represent simulations with ISR, the dashed lines represent collisions without ISR. The distributions are normalized to one.

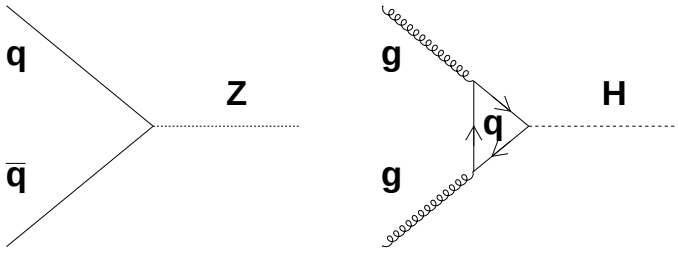

(a) $q\bar{q} \to Z$ (b) $gg \to H$

Figure 9: The two processes investigated in the `Pythia8` simulations.

2 Unintegrated parton density functions

As mentioned before, the transverse momentum of the partons is of great importance if one wishes to calculate correct kinematic values. In this section a closer look is given at different methods to calculate such transverse momentum distributions. The various methods used to calculate the unintegrated parton density function are explained. Results are shown at the end of in section (2.4).

The unintegrated parton densities are calculated from `Pythia8` collision simulations, `KMR` calculations starting from an integrated parton density functions and `CCFM` calculations.

2.1 `Pythia8`

`Pythia8` is a particle collision simulator. The user can choose which processes and effects he allows to occur, which particles can participate, at what energy the collision happens,... For each collision between two particles a list of created particles and their kinematic values is created. The user can use this list to calculate the kinematic values of the actual parton-parton collision. Since `Pythia8` doesn't provide a simple way of calculating these values, a program was written to calculate them. The outline of this program can be found in the appendix B.

Two different collisions have been investigated: the collision of a quark and an antiquark of the same flavour to a Z boson (figure 9a), and the collision of two gluons to a Higgs boson (figure 9b). From the first process we are able to determine a quark density function per flavour, from the second process we can extract a gluon density function. Note that the gluons are massless: they cannot create a Higgs boson directly, since the Higgs only interacts with massive particles. The gluons interact via a virtual quark loop: gluons can interact with quarks, and quarks can interact with the Higgs as they have mass. A Higgs boson is more likely to couple with heavier particles than with lighter particles, so the loop will most likely contain the very heavy top quark.

From a series of simulated collisions one can obtain a four dimensional histogram N_{ev} containing the transverse momentum of both partons $(k_{T,1}, k_{T,2})$ and their x value (x_1, x_2). This is a convolution of the parton density functions p:

$$N_{ev}(x_1, k_{T,1}, x_2, k_{T,2}) = q_1(x_1, k_{T,1}) \cdot q_2(x_2, k_{T,2}) \cdot \hat{\sigma}(x_1, k_{T,1}, x_2, k_{T,2}) \quad (26)$$

where $\hat{\sigma}$ is the cross section for the collision at parton level: the actual parton-parton to boson interaction.

If the cross section is known, we can continue with an integration over all kinematic values of the second parton:

$$\int dk_{T,1} dx_1 \frac{N_{ev}}{\hat{\sigma}(Q^2)} = q_1(x_1, k_{T,1}, Q^2) \quad (27)$$

where $q_1(x_1, k_{T,1}, Q^2)$ is the unintegrated parton density function.

2.1.1 Kinematics

The gauge boson created in the parton-parton collisions has a very specific mass which imposes certain kinematic constraints on the properties of the colliding partons:

$$\begin{aligned} Q^2 &= s \cdot x_1 \cdot x_2 & (28) \\ &= M^2 & (29) \end{aligned}$$

The first line shows that the available four-momentum squared depends on the four-momentum fractions of the two colliding partons (x_1, x_2) and the centre-of-mass collision energy (s). The second line means that all four-momentum squared from the two partons has to be used in the creation of the new boson with mass M. A gauge boson can only be created if the combined energy of the partons is high enough. This leads to a minimum value of x: if one parton has a very low value for x_1 the other parton needs to have a very large x_2. Since all x values are between 0 and 1, there is an upper bound on x_2 and thus a lower bound for x_1. In these collisions the lower bound will be around $x = 10^{-4}$. Because of this it only makes sense to compare `Pythia8`'s values with other values in the range above $10^{-2.5}$: at lower x the extracted $a(x)$ decreases rapidly whereas one would expect it to increase.

The mass of the created boson is not a fixed value but rather a distribution around the real mass value of M_r, which is due to the virtuality of the particle (as discussed in the introduction). It is distributed following the Breit-Wigner distribution:

$$BW\left(\sqrt{Q^2}\right) = \frac{1}{2\pi} \frac{\Gamma}{(\sqrt{Q^2} - M_r)^2 + \Gamma^2/4}. \quad (30)$$

Γ is called the decay-width and is expressed in GeV. In the following simulations, the mass of the Z-boson and the Higgs boson are stored in a histogram. A fit to this histogram returns the values of M_r and Γ. Note that the gauge boson will decay shortly after being created, and thus lives short enough to allow for a slightly different mass.

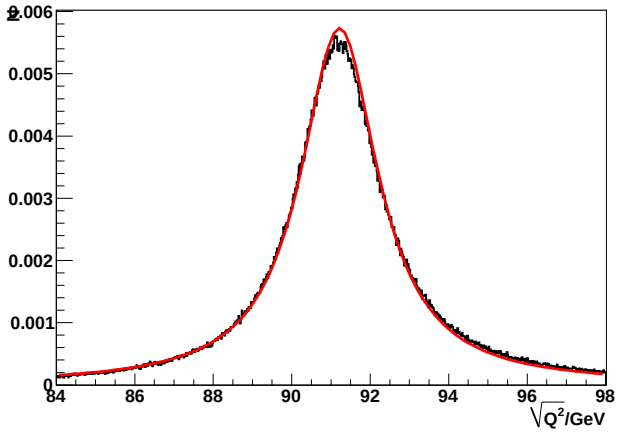

Figure 10: Fit of the Breit-Wigner function to the mass distribution of the Z-boson in `Pythia8`.

2.1.2 Z-boson

The cross section for a quark-antiquark to Z-boson collision is:

$$\hat{\sigma} = \frac{8\pi}{3}\frac{G_F M_Z}{\sqrt{2}}(g_a^2 + g_v^2)BW\left(\sqrt{Q^2}\right). \tag{31}$$

The different factors in the expression above are:

$$G_F = 1.1 \cdot 10^{-5}\ \text{GeV}^{-2} \tag{32}$$

$$(g_a^2 + g_v^2) = \frac{1}{8}\left(1 - 4|e_q|\sin^2\vartheta_w + 8e_q^2\sin^4\vartheta_w\right) \tag{33}$$

$$\sin^2\vartheta_w \approx 0.23. \tag{34}$$

G_F is the Fermi constant, ϑ_w is the Weinberg mixing angle and e_q is the quark charge.

This fit can be seen in figure 10.[9] The values of M_Z and Γ_Z as used by `Pythia8` are

$$M_Z = 91.2\ \text{GeV} \pm 1.6\ \text{GeV} \tag{35}$$

$$\Gamma_Z = 2.50\ \text{GeV} \pm 0.15\ \text{GeV} \tag{36}$$

From the simulation five different unintegrated parton density functions can be calculated: one for each flavour. The top quark is too heavy and does not appear in `Pythia8` simulations. It is not possible to choose which flavour the colliding quarks in the simulation have.

[9] It has to be noted that the distribution seen in figure 10 is in fact the Breit-Wigner distribution with an extra factor c. This factor describes the normalisation of the histogram but does not have any influence on the values of M or Γ.

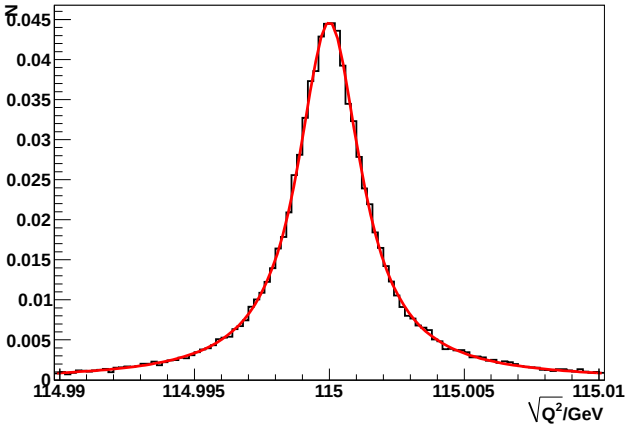

Figure 11: Fit of the Breit-Wigner function to the mass distribution of the Higgs boson in `Pythia8`.

2.1.3 Higgs boson

The cross section for the Higgs boson from gluon-gluon fusion is:

$$\hat{\sigma} = \frac{G_F \pi}{32\sqrt{2}} \left(\frac{\alpha_s}{\pi}\right)^2 |\eta|^2 \tau \frac{d\mathcal{L}_{gg}}{d\tau} \tag{37}$$

with

$$\eta = \frac{1}{3} \tag{38}$$

and

$$\tau \frac{d\mathcal{L}_{gg}}{d\tau} = 1. \tag{39}$$

The Breit-Wigner distribution is (30), and as with the Z-boson, a Breit-Wigner curve can be fitted to the Higgs boson mass distribution (figure 11). The values of M_H and Γ_H as used by `Pythia8` are

$$M_H = 115.0000 \text{ GeV } \pm 2.0 \cdot 10^{-3} \text{ GeV} \tag{40}$$

$$\Gamma_H = 2.8 \text{ MeV } \pm 4.45 \text{ MeV} \tag{41}$$

2.2 Kimber, Martin and Ryskin method

2.2.1 `KMR` Integrals

The unintegrated parton density function [9] [10] can be calculated using the integrated pdf and the *survival probability* $T_a(k_t, \mu)$. $T_a(k_t, \mu)$ is the probability that parton a with transverse momentum k_t does not emit anything in the evolution of the parton density function up to scale μ. For the comparing

[10] Please note that here we explicitly write $xa\left(\frac{x}{z}, k_t^2\right)$ whereas [9] uses $a\left(\frac{x}{z}, k_t^2\right)$ and assumes $a = xq$ or $a = xg$.

calculations in this thesis, we choose $\mu^2 = M_Z^2$ for quarks and $\mu^2 = M_H^2$ for gluons.

T_a is given by

$$T_a(k_t, \mu) = exp\left(- \int_{k_t^2}^{\mu^2} \frac{\alpha_s(k_t'^2)}{2\pi} \frac{dk_t'^2}{k_t'^2} \sum_{a'} \int_{z_{\min}}^{z_{\max}} P_{a'a}(z') dz' \right). \quad (42)$$

Because T_a is an exponential function, it in fact sums over all possible times splittings can occur. Due to the integral over z' T_a also accounts for all possible sizes z of these splittings. This can be used as follows to calculate the unintegrated parton density function

$$xf_a(x, k_t^2, \mu^2) = \frac{T_a(k_t, \mu)}{k_T^2} \sum_{a'=q,g} \left[\frac{\alpha_s}{2\pi} \int_x^{1-\Delta} P_{aa'}(z) x a' \left(\frac{x}{z}, k_t^2 \right) dz \right]. \quad (43)$$

f_a can be interpreted as follows: the probability to find a parton a' with energy-momentum fraction $\frac{x}{z}$ at scale k_T^2. This parton then experiences a splitting of size z and emits a parton a: this continues with energy-momentum fraction $\frac{x}{z} z = x$. T_a gives the probability that the parton a does not split any further in the evolution from k_T^2 to μ^2. If a does not emit anything, it will keep its x and k_T values up to scale μ^2. The explicit expressions for gluons and quarks are:

$$\begin{aligned} xf_g(x, k_t^2, \mu^2) &= \frac{T_g(k_t, \mu)}{k_T^2} \frac{\alpha_s}{2\pi} \int_x^{1-\Delta} \left(P_{gg}(z) x g\left(\frac{x}{z}, k_T^2 \right) + \sum_i P_{gq} x q_i \left(\frac{x}{z}, k_T^2 \right) \right) dz \\ xf_{q_i}(x, k_t^2, \mu^2) &= \frac{T_q(k_t, \mu)}{k_T^2} \frac{\alpha_s}{2\pi} \int_x^{1-\Delta} \left(P_{q_i g}(z) x g\left(\frac{x}{z}, k_T^2 \right) + P_{qq} x q_i \left(\frac{x}{z}, k_T^2 \right) \right) dz \end{aligned}$$

where the sum goes over all quark and antiquark flavours. Note that where the gluon splits, it can split into a gluon or all quark flavours. The quark can only emit a gluon or a quark of the same flavour.

The constant Δ is an arbitrary cut-off to prevent possible divergencies in splitting functions. $1 - \Delta$ can be interpreted as the maximum z-value of an emission that will be detectable: if z is higher, $1 - z$ will become so low that the two particles can not be distinguished and thus remain one particle. Δ is arbitrary and is chosen to be equal to cut-off ε, see below. Note that any arbitrary cut-off will be compensated by adjusting the bare parton distribution, see section 1.3.4.

2.2.2 Parton density functions and `LHAPDF`

The parton density functions used in the formulas above are taken from the `LHAPDF` libraries [10]. The pdfsets `Pythia8` uses by default are `cteq5l`, and there is the possibility of using the `GRV94L` instead. It is also possible to couple an external library to `Pythia8`, which makes it possible to acces many different pdfsets.

Since `Pythia8` works with `cteq5l` by default, this set will be used in our `KMR` calculations. The pdf is used via the $xfx\left(x, Q^2, flavour\right)$ command in `Pythia8`.

In the definitions above the transverse momentum k_T^2 serves as the scale Q^2 for the integrated parton densities, not as an actual transverse momentum.

2.2.3 Integration of the pdf

We now turn to the integration of these pdf's according to equation (43). The splitting functions $P_{aa'}$ have a known analytical form, but the measured pdf's don't. We are forced to use Monte Carlo integration, see appendix C.

2.2.4 The T_q-factor

The last step in calculating the unintegrated parton density function is the calculation of the T_a-factor. Part of T_a can be calculated explicitly using some simplifications: the integration bounds on the dz integral are set to $z_{\min} = 1 - z_{\max}$. Using these simplifications we first calculate the analytical part of T_q, which is the integration over z:

$$\begin{aligned}
\sum_{a'=q,g} \int_{z_{\min}}^{z_{\max}} P_{a'q}(z)dz &= \int_{z_{\min}}^{z_{\max}} \left(P_{gq}(z) + P_{qq}(z)\right) dz \\
&= \int_{z_{\min}}^{z_{\max}} \left(\frac{4}{3}\frac{1+z^2}{1-z} + \frac{4}{3}\frac{1+(1-z)^2}{z}\right) dz \\
&= \frac{8}{3}\int_{z_{\min}}^{z_{\max}} \frac{1+(1-z)^2}{z} dz \\
&= \frac{8}{3}\int_{z_{\min}}^{z_{\max}} \left(\frac{2}{z} - 2 + z\right) dz \\
&= \frac{8}{3}\left[2\ln z - 2z + \frac{z^2}{2}\right]_{z_{\min}}^{z_{\max}} \\
&= \frac{8}{3}\left[2\ln z - 2z + \frac{z^2}{2}\right]_{\varepsilon}^{1-\varepsilon} \\
&= \frac{8}{3}\left[2\ln\left(\frac{1-\varepsilon}{\varepsilon}\right) - 2(1-2\varepsilon) + \frac{(1-2\varepsilon+\varepsilon^2)-\varepsilon^2}{2}\right] \\
&= \frac{8}{3}\left[2\ln\left(\frac{1-\varepsilon}{\varepsilon}\right) - \frac{3}{2} + 3\varepsilon\right]
\end{aligned}$$

where in the last step we replaced $z_{\min}$ with the parameter ε. This expression depends on only one parameter, and is independant of any kinematic variable.

The second part of the exponent in (42) can in general not be solved analytically.

2.2.5 The T_g-factor

The T_g-factor is calculated analogous to the the T_q factor, with the difference that a gluon can split into a quark-antiquark pair with any flavour.

$$
\begin{aligned}
\sum_{a'=q,g} \int_{z_{\min}}^{z_{\max}} dz P_{a'g}(z) &= \int_{z_{\min}}^{z_{\max}} dz \left(P_{gg}(z) + N_f P_{qg}(z)\right) \\
\int_{z_{\min}}^{z_{\max}} dz P_{gg}(z) &= 6 \int_{z_{\min}}^{z_{\max}} dz \left(\frac{1-z}{z} + \frac{z}{1-z} + (1-z)z\right) \\
&= 6 \int_{z_{\min}}^{z_{\max}} dz \left(\frac{1}{z} - 1 + z - z^2\right) + 6 \int_{z_{\min}}^{z_{\max}} dz \frac{z}{1-z} \\
&= 6 \left(\ln(z) - z + \frac{z^2}{2} - \frac{z^3}{3}\right)\Big|_{z_{\min}}^{z_{\max}} - 6 \int_{y_{min}}^{y_{max}} dy \frac{1-y}{y} \\
&= 6 \left(\ln\left(\frac{z_{\max}}{z_{\min}}\right) + (z_{\max} - z_{\min}) + \frac{z_{\max}^2 - z_{\min}^2}{2} - \frac{z_{\max}^3 - z_{\min}^3}{3}\right) \\
&\quad -6 \left(\ln\left(\frac{1-z_{\max}}{1-z_{\min}}\right) + ((1-z_{\max}) - (1-z_{\min}))\right)
\end{aligned}
$$

This is the most general expression for this integral. We now use:

$$
\begin{aligned}
z_{\max} &= 1 - \varepsilon \qquad (44) \\
z_{\min} &= \varepsilon \qquad (45)
\end{aligned}
$$

which results in

$$
\begin{aligned}
\int_{\varepsilon}^{1-\varepsilon} dz P_{gg}(z) &= 6 \left(\ln\left(\frac{1-\varepsilon}{\varepsilon}\right) + ((1-\varepsilon) - \varepsilon) + \frac{(1-\varepsilon)^2 - \varepsilon^2}{2} - \frac{(1-\varepsilon)^3 - \varepsilon^3}{3}\right) \\
&\quad -6 \left(\ln\left(\frac{1-(1-\varepsilon)}{1-\varepsilon}\right) + ((1-(1-\varepsilon)) - (1-\varepsilon))\right) \\
&= 6 \left(\ln\left(\frac{1-\varepsilon}{\varepsilon}\right) + (1-2\varepsilon) + \frac{1-2\varepsilon}{2} - \frac{1-3\varepsilon+3\varepsilon^2-\varepsilon^3}{3}\right) \\
&\quad +6 \left(\ln\left(\frac{1-\varepsilon}{\varepsilon}\right) + 2\varepsilon - 1\right) \\
&= 12 \ln\left(\frac{1-\varepsilon}{\varepsilon}\right) + 1 - 6\varepsilon^2 + 2\varepsilon^3. \qquad (46)
\end{aligned}
$$

The quark part of the integral is:

$$\begin{aligned}
\int_{z_{\min}}^{z_{\max}} dz P_{qg}(z) &= \frac{1}{2}\int_{z_{\min}}^{z_{\max}} dz\left(z^2+(1-z)^2\right) \\
&= \frac{1}{2}\int_{z_{\min}}^{z_{\max}} dz\left(2z^2-2z+1\right) \\
&= \frac{1}{2}\left(\frac{2z^3}{3}-z^2+z\right)\Bigg|_{z_{\min}}^{z_{\max}} \\
&= \frac{1}{2}\left(2\frac{z_{\max}^3-z_{\min}^3}{3}-(z_{\max}^2-z_{\min}^2)+(z_{\max}-z_{\min})\right) \quad (47) \\
&= \frac{1}{2}\left(2\frac{(1-\varepsilon)^3-\varepsilon^3}{3}-((1-\varepsilon)^2-\varepsilon^2)+((1-\varepsilon)-\varepsilon)\right) \\
&= \frac{1}{2}\left(2\frac{1-3\varepsilon+3\varepsilon^2-2\varepsilon^3}{3}+(2\varepsilon-1)+(1-2\varepsilon)\right) \\
&= \frac{1}{3}-\varepsilon+\varepsilon^2-\frac{2}{3}\varepsilon^3 \quad (48)
\end{aligned}$$

where after (47) we entered the same integral bounds as above. (47) is the most general solution for this integral.

Now combining (46) and (48), we get:

$$\begin{aligned}
\int_{z_{\min}}^{z_{\max}} dz\left(P_{gg}(z)+N_f P_{qg}(z)\right) &= 12\ln\left(\frac{1-\varepsilon}{\varepsilon}\right)+1-6\varepsilon^2+2\varepsilon^3+N_f\left(\frac{1}{3}-\varepsilon+\varepsilon^2-\frac{2}{3}\varepsilon^3\right) \\
&= 12\ln\left(\frac{1-\varepsilon}{\varepsilon}\right)+\left(1+\frac{N_f}{3}\right)-N_f\varepsilon+(N_f-6)\varepsilon^2+\left(2-\frac{N_f 2}{3}\right)\varepsilon^3 \quad (49)
\end{aligned}$$

The cut-offs Δ and ε are arbitrary. All emission with z beyond one of the cuts will be treated as a part of the parton, not as a real emission.

2.3 `CCFM` unintegrated gluon density function

The Catani-Ciafaloni-Fiorani-Marchesini method [4] calculates the unintegrated gluon density function using *angular ordering*. If a gluon splits at a scale $q_(i-1)$ with a splitting size of $z_{(i-1)}$, then the next scale of splitting q_i will be:

$$q_i > q_{(i-1)} z_{(i-1)}. \quad (50)$$

These calculations were not a part of this thesis but the `CCFM` values are used as an extra test to compare our own results with.

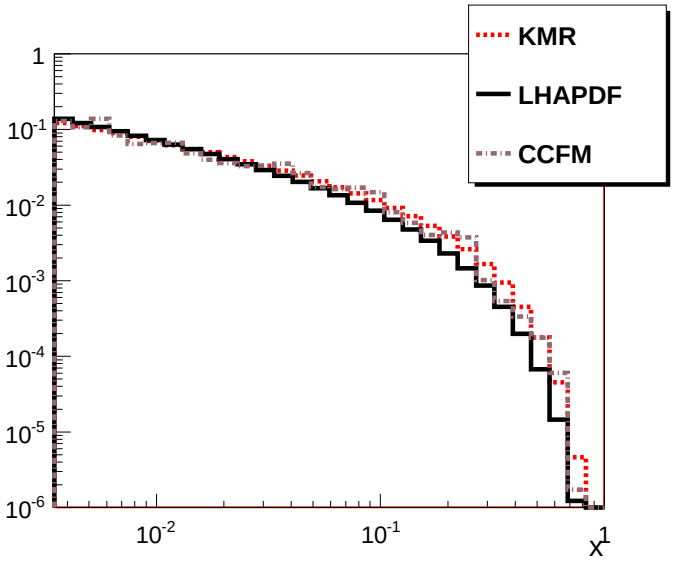

Figure 12: Comparison of integrated gluon density functions $xg(x)$ obtained via different methods. Distributions normalized to one.

2.4 Results

The results for the different methods are compared. In order to be able to compare the unintegrated functions with the `LHAPDF` data, the updf's are integrated over k_T.

A first discovery is that for all partons there is very little difference between the parton density functions of `Pythia8` with and without ISR. This means that, at least in `Pythia8` simulations, the inclusion of possible high transverse momenta does not affect the distribution in x.

2.4.1 Gluon density functions

In figure 12 the different integrated gluon density functions are shown, all normalized to one. Because of this, the plots can be compared for shape but not for absolute value.

The `KMR` and `CCFM` results have the same shape as the `LHAPDF` (`cteq5l` dataset), but at high x-values they decrease slower than the `LHAPDF` values. This may be due to quarks, which are unaccounted for in these calculations.

In figure 13 it can be seen that if x decreases, $xg(x)$ will increase and decrease again. This is because of the constraint on the `Pythia8` simulations.

2.4.2 Quark density functions

In figures 14, 16, 18,20 and 22 the quark density functions calculated from different methods are compared. All these plots show the quarks and not the antiquarks. For the strange, charm and bottom quark the quark- and antiquark density functions will be the same: they are only present as seaquarks and are thus created from gluons splitting into a quark-antiquark pair. The gluon does

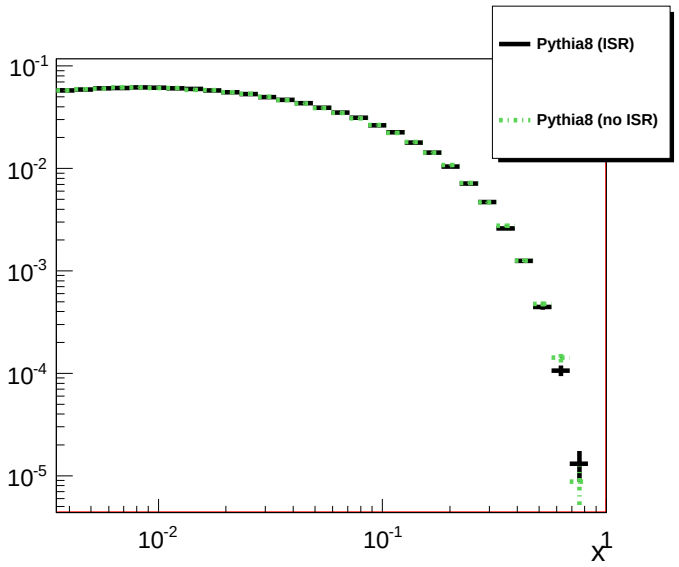

Figure 13: Comparison of integrated gluon density functions $xg(x)$ obtained via `Pythia8` methods. Distributions normalized to one.

not treat quark and antiquark in a different way, so the kinematic effects on both are the same and thus they have a similar distribution.

The up and down quark however are also present in the proton as valence quarks. These valence quarks will carry a significant portion of the proton's four-momentum and have high x-values. The bumps in the $xg(x)$ distributions around $x \approx 1/3$ are the valence quarks. Notice that the bumps are not located at $x \approx 1/3$ but lie at a slightly lower x: at a high scale the proton contains much more particles, all particles that take their four-momentum from the valence quarks.

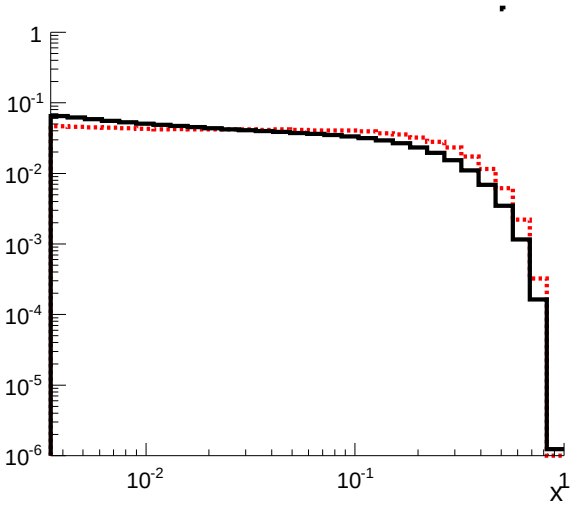

Figure 14: Comparison of integrated down quark density functions $xd(x)$ obtained via `LHAPDF` (full black line) and `KMR` (dashed red line).

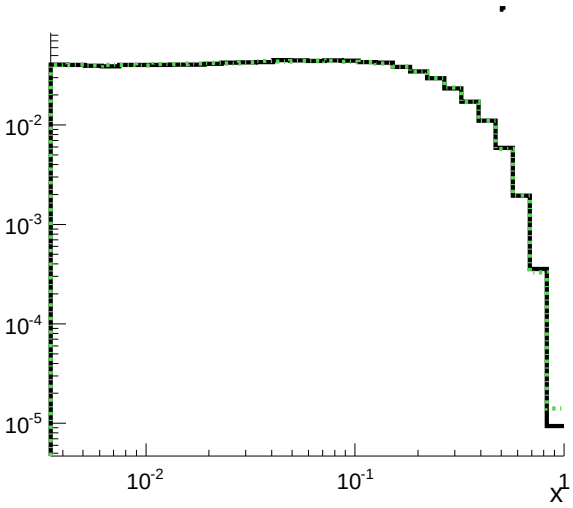

Figure 15: Comparison of integrated down quark density functions $xd(x)$ obtained via `Pythia8` without ISR (full black line) and `Pythia8` with ISR (dashed green line).

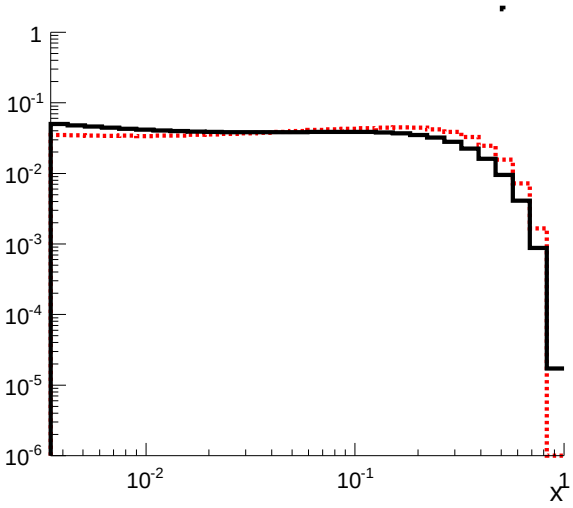

Figure 16: Comparison of integrated up quark density function $xu(x)$s obtained via `LHAPDF` (full black line) and `KMR` (dashed red line).

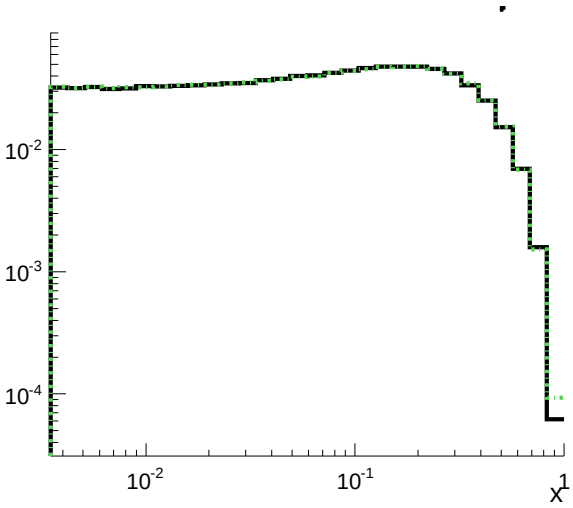

Figure 17: Comparison of integrated up quark density functions $xu(x)$ obtained via `Pythia8` without ISR (full black line) and `Pythia8` with ISR (dashed green line).

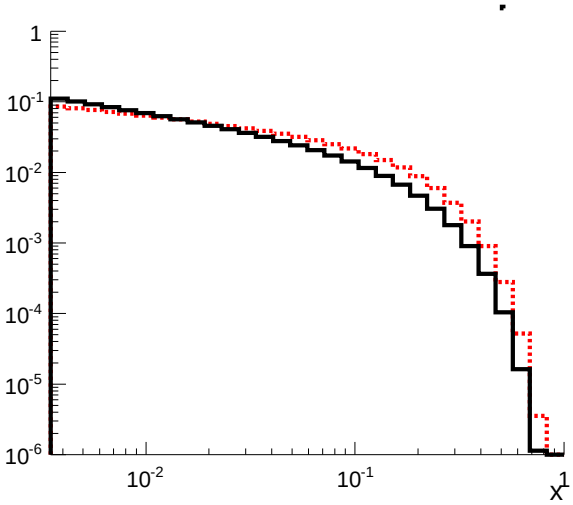

Figure 18: Comparison of integrated strange quark density function $xs(x)$s obtained via `LHAPDF` (full black line) and `KMR` (dashed red line).

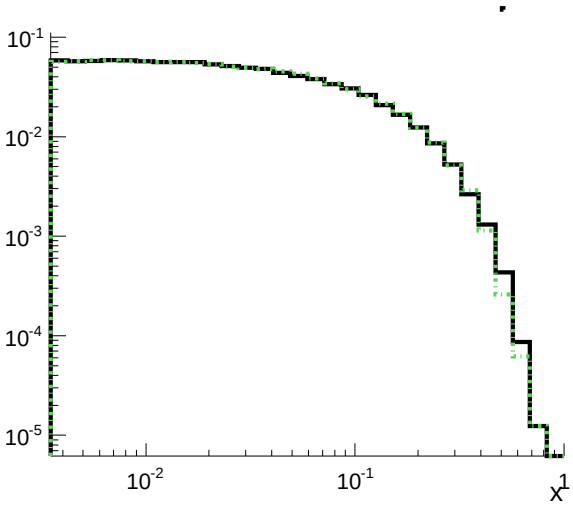

Figure 19: Comparison of integrated strange quark density functions $xs(x)$ obtained via `Pythia8` without ISR (full black line) and `Pythia8` with ISR (dashed green line).

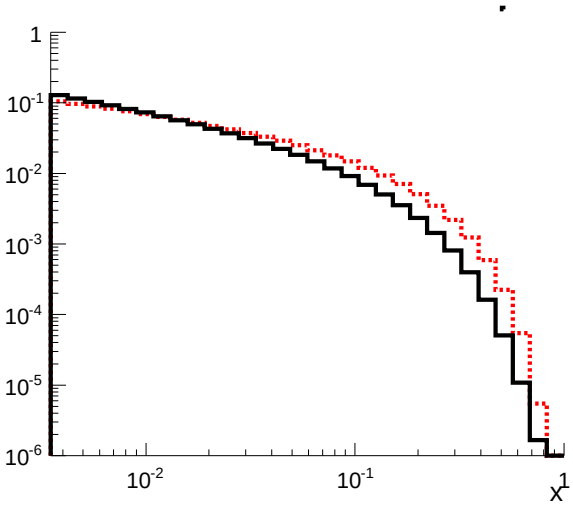

Figure 20: Comparison of integrated charm quark density functions $xc(x)$ obtained via `LHAPDF` (full black line) and `KMR` (dashed red line).

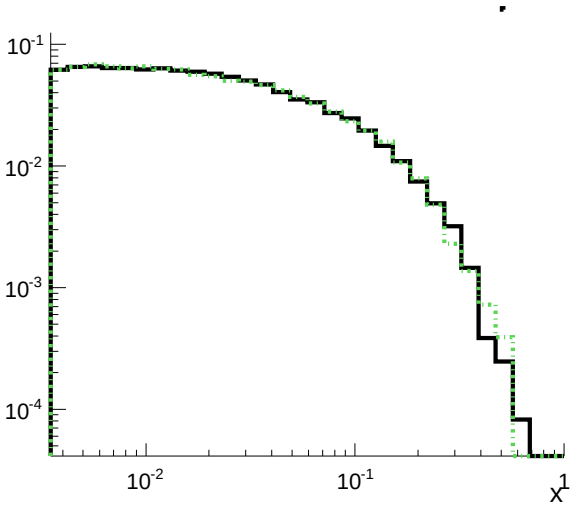

Figure 21: Comparison of integrated charm quark density functions $xc(x)$ obtained via `Pythia8` without ISR (full black line) and `Pythia8` with ISR (dashed green line).

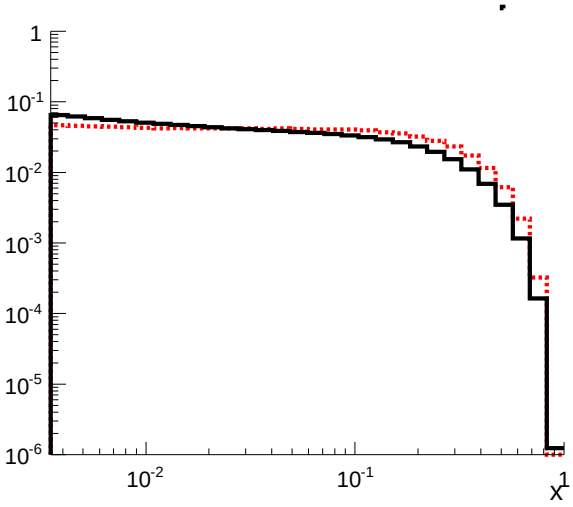

Figure 22: Comparison of integrated bottom quark density functions $xb(x)$ obtained via `LHAPDF` (full black line) and `KMR` (dashed red line).

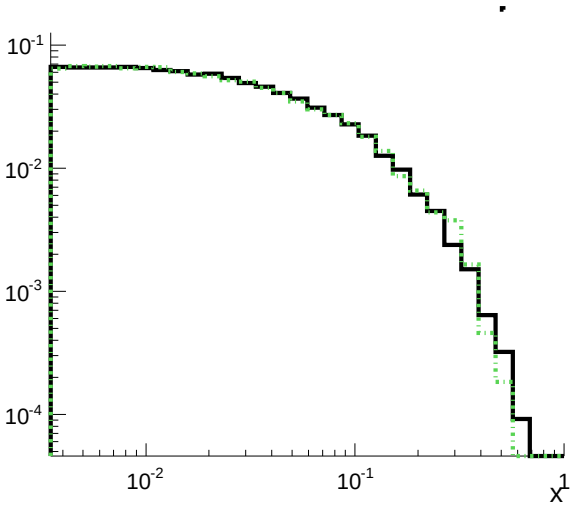

Figure 23: Comparison of integrated bottom quark density functions $xb(x)$ obtained via `Pythia8` without ISR (full black line) and `Pythia8` with ISR (dashed green line).

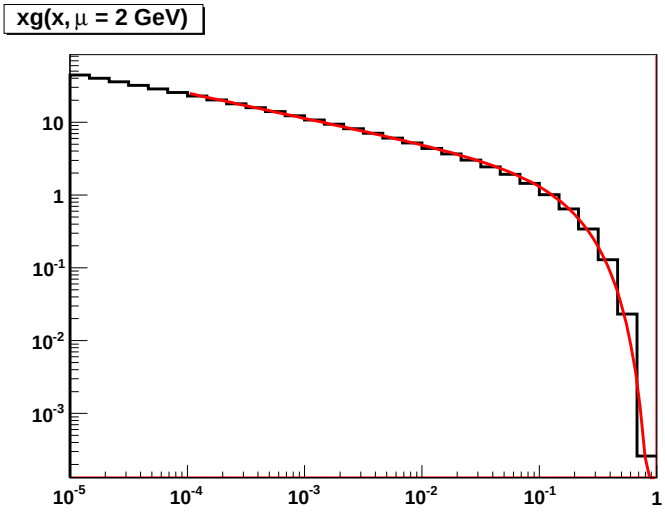

Figure 24: The gluon density function from the `cteq5l` set as a function of x, fitted to function (51). The scale μ is set to 2 GeV. The red line is the fit, the black line the `LHAPDF` data.

3 Evolution of gluon density functions

In this section we take a closer look at the gluon density function and its evolution between two scales. The scales between which the evolution takes place are named t_0 and t_f. Note that these scales are expressed in GeV^2, just as the scale Q^2.

In section 3.1 the general procedure for evolving gluon density functions is explained, while in 3.2 some specific examples are looked at.

3.1 Evolution of the gluon density function

The starting distribution for the calculations is a fit to the `LHAPDF` [4] data. The analytical function

$$g(x, \mu = 2 \text{ GeV}) = ax^b(1-x)^c(1+dx)/x \tag{51}$$

is fitted to the data. The coefficients of this fit are:

$$\begin{aligned} a &= 1.041 \cdot 10^0 \\ b &= -3.456 \cdot 10^{-1} \\ c &= 4.934 \cdot 10^0 \\ d &= -5.537 \cdot 10^{-1}. \end{aligned} \tag{52}$$

In figure 24 the gluon density function $xg(x)$ from the `LHAPDF` data and the fit of this function are shown ($g(x)$ has been fitted but $xg(x)$ is shown). The evolution is done by using a Monte Carlo simulation process. Evolution from a lower scale t_0 to a higher scale t_f happens as follows.

- A random x_0-value is generated, and for this value $g(x_0, t_0)$ is calculated. This value represents the gluon that will be evolved.
- A random z-value is generated between $z_{\min} > 0$ and $z_{\max} < 1$ (cut-offs introduced to prevent divergence) following the $P_{gg}(z)$ function. This is the value of the momentum fraction that an emitted gluon will carry away. Note that this fraction z_1 does not depend on the scale t_1 at which the splitting occurs.
- To calculate the scale at which the gluon will split we need the Sudakov form factor Δ_s:

$$\Delta_s = \exp\left(-\int dz \int_{t_0}^{t_1} \frac{dq'}{q'} \frac{\alpha_s}{2\pi} P_{gg}(z)\right). \tag{53}$$

  Δ_s represents the probability that a gluon will not split between scales t_0 and t_1, and is thus very similar to T_a (42). The scale t_1 is generated following this probability distribution. q' is expressed in GeV.
- At scale t_1 the x value of the gluon is adjusted: $x_1 = x_0 z_1$. Since any z value is smaller than one, x_1 will be smaller than x_0: the gluon has lost some of its energy-momentum. The gluon density $g(x_0, t_0)$ does not change.
- Repeat this process now, using t_1 is the starting scale. Note the starting scale as t_{n-1} and the new scale of splitting as t_n. The size of splitting at t_n is z_n.
- If $t_n > t_f$ the gluon has passed the final scale of the evolution. Its x value after $n-1$ splittings between t_0 and t_f will be

$$x_f = x_{n-1} \tag{54}$$

$$= \prod_{i=1}^{n-1} z_i x_0. \tag{55}$$

  A histogram will represent $g(x, t_f)$. The value $g(x_0, t_0)$ is added to the histogram bin for x_{n-1}.
- This whole process is repeated N times, each time starting from a random x_0 value.

3.2 Evolution of the distribution

The most important factor in the evolution is the coupling strength $\alpha_s(\mu^2)$ and its scale μ^2. This can be either a constant, a transverse momentum (p_T) or a transverse momentum after splitting[11] ($p_T(1-z)$). For each of these situations the functions needed for the evolution will be calculated with following approximations[12]:

[11] The results for this last method were incorrect, so they have been left out of the main body of the thesis. The calculations can be found in the appendix.

[12] Exercise 4 solution `Pgg`: http://www.desy.de/~jung/qcd_and_mc_2010/QCD_and_MC_2010_%28Antwerp%29.html

- The splitting function is approximated:

$$P_{gg}(z) \approx 6\left(\frac{1}{z} + \frac{1}{1-z}\right). \tag{56}$$

- To avoid divergencies in the splitting function, we use following arbitrary bounds:

$$\begin{aligned} z_{\min} &= \varepsilon \\ z_{\max} &= 1-\varepsilon \\ \text{with: } \varepsilon &= 0.1 \end{aligned} \tag{57}$$

- z is generated following the distribution:

$$\tilde{P}_{gg}(z) = 6\frac{\alpha_s}{2\pi}\left(\frac{1}{z} + \frac{1}{1-z}\right). \tag{58}$$

- In the analysis performed here, we leave out the quark contributions: there are no gluons that originate from quarks, nor can a gluon split into a quark-antiquark pair in the evolution. Quark contributions do appear in reality, but are small enough to be neglected. This is especially true at low x, see section 1.4.

3.2.1 Fixed α_s

The first evolution will be done with a fixed value for the strong coupling:

$$\alpha_s = 0.1. \tag{59}$$

The Sudakov form factor is then an easy analytical integral, and we can generate a scale t_1 above t_0 according to the Sudakov form factor.

$$R = \exp\left[-\int dz \int_{t_0}^{t_1} \frac{dt}{t}\frac{1}{2}\frac{\alpha_s}{2\pi}P(z)\right] \tag{60}$$

$$= \exp\left[-\int dz P(z)\frac{1}{2}\frac{\alpha_s}{2\pi}\ln\left(\frac{t_1}{t_0}\right)\right] \tag{61}$$

$$-\ln R = \int dz P(z)\frac{1}{2}\frac{\alpha_s}{2\pi}\ln\left(\frac{t_1}{t_0}\right) \tag{62}$$

$$-\ln R\frac{4\pi}{\alpha_s\int dz P(z)} = \ln\left(t_1/t_0\right) \tag{63}$$

$$t_1 = t_0 R^{-4\pi/(\alpha_s\int dz P(z))} \tag{64}$$

where we used the substitution $q = t^{1/2}$, and R is a uniform random number between 0 and 1.

The z of the gluon emitted at t_1 is generated according to the $\tilde{P}_{gg}(z)$:

$$
\begin{aligned}
R' \int_{z_{\min}}^{z_{\max}} dz \tilde{P}_{gg}(z) &= \int_{z_{\min}}^{z} dz \tilde{P}_{gg}(z) && (65)\\
R' \int_{z_{\min}}^{z_{\max}} dz 6 \frac{\alpha_s}{2\pi} \left(\frac{1}{z} + \frac{1}{1-z} \right) &= \int_{z_{\min}}^{z} dz 6 \frac{\alpha_s}{2\pi} \left(\frac{1}{z} + \frac{1}{1-z} \right) && (66)\\
R' 2 \ln \left(\frac{1-\varepsilon}{\varepsilon} \right) &= \int_{z_{\min}}^{z} dz \frac{1}{z} + \int_{z_{\min}}^{z} dz \frac{1}{1-z} && (67)\\
&= \int_{z_{\min}}^{z} dz \frac{1}{z} - \int_{1-z_{\min}}^{1-z} dz' \frac{1}{z'} && (68)\\
&= \ln \left(\frac{z}{z_{\min}} \right) - \ln \left(\frac{1-z}{1-z_{\min}} \right) && (69)\\
&= \ln \left(\frac{z(1-z_{\min})}{z_{\min}(1-z)} \right) && (70)
\end{aligned}
$$

where we used $z' = 1 - z$. From this equation we obtain a value for z:

$$
\begin{aligned}
\left(\frac{1-\varepsilon}{\varepsilon} \right)^{2R'} &= \frac{z(1-z_{\min})}{z_{\min}(1-z)} && (71)\\
z_{\min}(1-z) \left(\frac{1-\varepsilon}{\varepsilon} \right)^{2R'} &= z(1-z_{\min}) && (72)\\
z(1-z_{\min}) + z z_{\min} \left(\frac{1-\varepsilon}{\varepsilon} \right)^{2R'} &= z_{\min} \left(\frac{1-\varepsilon}{\varepsilon} \right)^{2R'} && (73)\\
z &= \frac{z_{\min} \left(\frac{1-\varepsilon}{\varepsilon} \right)^{2R'}}{(1-z_{\min}) + z_{\min} \left(\frac{1-\varepsilon}{\varepsilon} \right)^{2R'}} && (74)\\
&= \frac{\varepsilon \left(\frac{1-\varepsilon}{\varepsilon} \right)^{2R'}}{(1-\varepsilon) + \varepsilon \left(\frac{1-\varepsilon}{\varepsilon} \right)^{2R'}}. && (75)
\end{aligned}
$$

In figure 25 the distributions of the number of times emission occurs and the scales at which this happens, are shown. It is clear that the highest probability for emission can be found at the lower scale.

The number of gluons emitted is shown in figure (a): a gluon is most likely not to change between scales $\mu = 2$ GeV and $\mu = 100$ GeV. Emission is possible, but chance of emission decreases with an increasing number of emitted gluons.

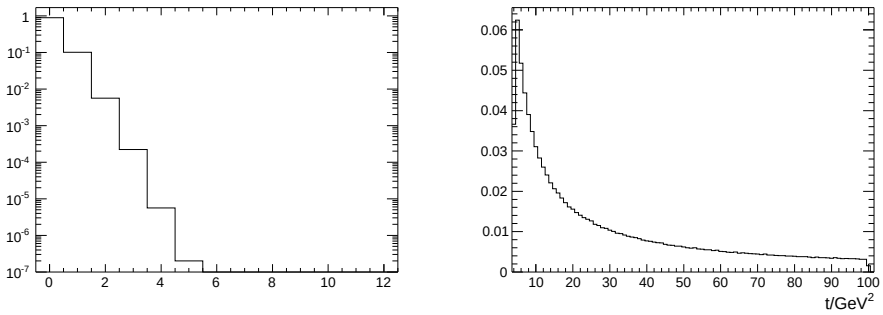

(a) Number of emissions

(b) Scale of emissions

Figure 25: The distributions of number of times, and the scales at which emissions occur. Evolution between 4 GeV^2 and 100 GeV^2. Both distributions are normalized to one.

3.2.2 Non-fixed α_s: $Q = q_t$

The scale used is the scale q_t^2 at which the gluon radiation takes place:

$$t_0 < q_t^2 < t_f. \tag{76}$$

The big difference with the section above is that the evolution up to a higher scale is done with a variable coupling. The most important consequence of this lies in the calculation of the Sudakov form factor. Different scales are used for the coupling. The analytical expression for the strong coupling is (24).

Entering this scale in the coupling (24) in the Sudakov form factor yields

$$\ln \Delta_s = -\int dz P_{gg}(z) \int \frac{dt}{t} \frac{\alpha_s(q_t)}{2\pi}. \tag{77}$$

t is a scale with unit GeV^2, so we can replace it with q_t^2 which has the same unit.

$$\begin{aligned}
\ln \Delta_s &= -\int dz P_{gg}(z) \int \frac{dq_t^2}{q_t^2} \frac{\alpha_s(q_t)}{2\pi} && (78)\\
&= -\int dz P_{gg}(z) \int \frac{dq_t^2}{q_t^2} \frac{1}{\ln(q_t^2/\Lambda^2)} \frac{12\pi}{2\pi(33-2n_f)} && (79)\\
&= -\int dz P_{gg}(z) \int \frac{dQ}{Q} \frac{1}{\ln(Q)} \frac{6}{(33-2n_f)} && (80)\\
&= -\int dz P_{gg}(z) \int \frac{du}{u} \frac{6}{(33-2n_f)} && (81)\\
&= -\int dz P_{gg}(z) \ln\left(\frac{u_{\max}}{u_{\min}}\right) \frac{6}{(33-2n_f)} && (82)\\
&= -\int dz P_{gg}(z) \ln\left(\frac{\ln(Q_{\max})}{\ln(Q_{\min})}\right) \frac{6}{(33-2n_f)} && (83)\\
&= -\int dz P_{gg}(z) \ln\left(\frac{\ln(t_{\max}/\Lambda^2)}{\ln(t_{\min}/\Lambda^2)}\right) \frac{6}{(33-2n_f)} && (84)
\end{aligned}$$

where we have used substitutions: $\ln(t/\Lambda^2) = Q$ and $u = \ln(Q)$.

Having found the expression for this integral, we can proceed to obtain the value of $t_{\max} = t$.

$$\begin{aligned}
\ln \Delta_s &= C \ln\left(\frac{\ln(t/\Lambda^2)}{\ln(t_{\min}/\Lambda^2)}\right) && (85)\\
\ln\left(\Delta_s^{1/C}\right) &= \ln\left(\frac{\ln(t/\Lambda^2)}{\ln(t_{\min}/\Lambda^2)}\right) && (86)\\
\ln(t_{\min}/\Lambda^2) &= \ln(t/\Lambda^2) && (87)\\
\left(\frac{t_{\min}}{\Lambda^2}\right)^{\Delta_s^{1/C}} \Lambda^2 &= t && (88)
\end{aligned}$$

where we have collected all constants in one constant C:

$$\begin{aligned}
C &= -\frac{6}{(33-2n_f)} \int dz P_{gg}(z) && (89)\\
&= -\frac{6}{(33-2n_f)} 2 \ln\left(\frac{z_{\max}}{z_{\min}}\right) && (90)
\end{aligned}$$

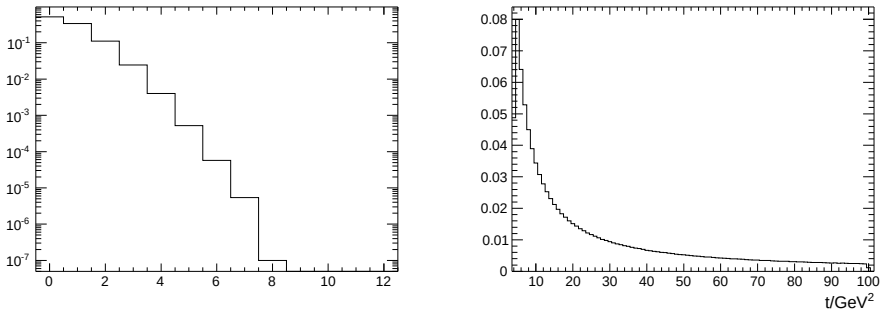

(a) Number of emissions

(b) Scale of emissions

Figure 26: The distributions of number of times, and the scales at which emissions occur. Evolution between 4 GeV^2 and 100 GeV^2. Both distributions are normalized to one.

In equation (88) we can now replace Δ_s with a uniform random number R with value between 0 and 1, so that t becomes a random number following the Sudakov distribution.

The z-value of the emitted gluon can be calculated with the same equation (75) used in the constant α_s scenario. α_s does not depend on z, and drops out of the equation without any problem.

We can now compare the difference in behaviour of emissions between the constant and variabel coupling constant scenarios. In figure 26 we can see that between 4 GeV^2 and 100 GeV^2 a gluon most likely will emit no or just one gluon. The probability of emission at a certain scale is very similar to the scenario of the constant coupling: splitting is most probable to happen at a low scale. The only notable difference is the peak: for the variable coupling constant it is slightly higher.

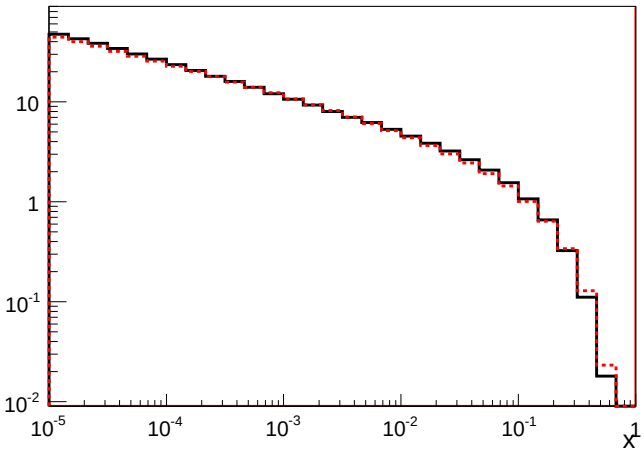

Figure 27: Comparison of the histogram taken from $xg(x)$ (full black line) and the LHAPDF data (red dashed line), at scale $\mu = 4$ GeV^2. The starting distribution is the same for all evolutions.

3.3 Results

In this section the results for the various evolution methods are compared with eachother. Also compared are the two-dimensional unintegrated parton densities: an evolved updf is compared with KMR.

3.3.1 Integrated parton densities

In figure 27 the gluon distributions $xg(x)$ are shown at scale $\mu = 2$ GeV: one histogram is taken from the LHAPDF library (which returns $xg(x)$, so this data is divided by x), the other is the distribution (51). Starting from this second distribution, the gluon density is evolved (as described in the previous sections). The results are shown in figures 28, 29 and 30, together with the LHAPDF data.

3.3.2 Unintegrated parton densities

As can be seen in the section above, the result the closest to the LHAPDF values is the evolution using p_T as a scale for α_s. This evolution is now used to calculate the unintegrated parton density and compared to the KMR values. The unintegrated parton density only uses gluons. We check if KMR returns a similar value using only gluons: we leave out all gluons coming from quarks (P_{gq}) and gluons will not split into two quarks (P_{qg}).

The calculation and evolution of an unintegrated parton density starts from an integrated parton density. The evolution begins at t_0 with transverse momentum $k_{T,0} = 0$. Evolving this parton density function happens in the same way as evolving an integrated parton density. The only difference is that the k_T of the gluon also develops. At each splitting, the components of k_T are adjusted:

$$k_x^{(n)} = k_x^{(n-1)} + \sqrt{t}\cos\varphi^{(n)} \quad (91)$$

$$k_y^{(n)} = k_y^{(n-1)} + \sqrt{t}\sin\varphi^{(n)} \quad (92)$$

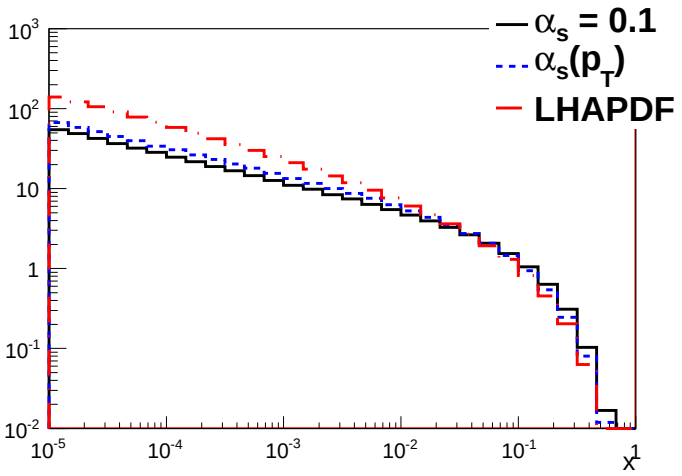

Figure 28: Comparison of the `LHAPDF` data and the evolved $xg(x)$ for different values of α_s, at scale $\mu^2 = 60$ GeV^2.

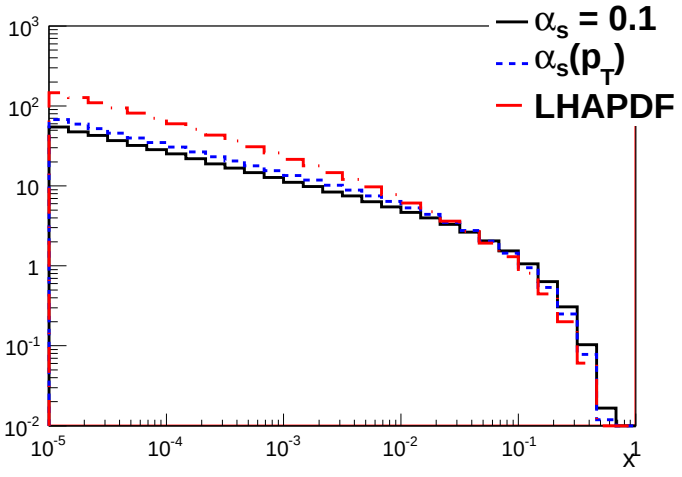

Figure 29: Comparison of the `LHAPDF` data and the evolved $xg(x)$ for different values of α_s, at scale $\mu^2 = 70$ GeV^2.

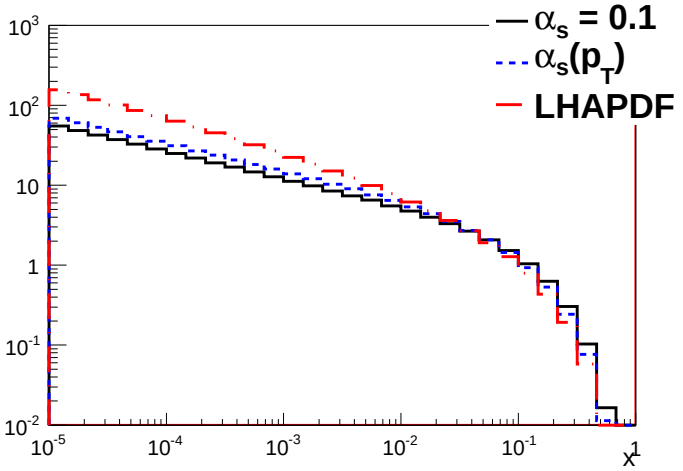

Figure 30: Comparison of the LHAPDF data and the evolved $xg(x)$ for different values of α_s, at scale $\mu^2 = 90$ GeV^2.

where $k^{(n)}$ notes the momentum after the nth splitting. $\varphi^{(n)}$ is a random angle between 0 and 2π.

When the gluon has been evolved up to the final scale t (with $n-1$ splittings happening between t_0 and t), the value x_{n-1} and $k_T^{(n-1)}$ are stored in a 2D histogram. The evolved updf and the KMR updf are shown in figures 35 and 36. Both distributions show more gluons at low x, but the KMR distribution shows nearly no low k_T^2 gluons while the evolved distribution shows nearly no high k_T^2 gluons. It should be noted that few emissions take place between $t_0 = 4$ GeV^2 and $t_1 = 90$ GeV^2, so a number of gluons will either not develop any transverse momentum.

The unintegrated parton densities from evolution and KMR look similar but have some essential differences. The KMR distribution at 60 and 70 GeV^2 (plots 31 and 33) has a peak in k_T^2 which is clearly different from 0, while the peak for the evolved distributions lies at $k_T^2 = 0$, for all values of x. Also: the KMR distribution is much more smeared out than the evolved distribution: gluons can have values $k_T^2 = Q^2$.

3.4 Calculation of F_2

In this section both integrated and unintegrated parton density functions are used to calculate the structure function of the proton. All calculations are compared with the HERA values of F_2 [14].

The comparison of calculated and measured structure function values is a test for the theory and methods used when evolving parton density functions..

From the HERA data all points with $x \leq 10^{-2}$ and $Q^2 \geq 5$ GeV^2 are taken. These points lie in the gluon dominated region, and it should be possible to calculate a reasonable value for F_2^g with only the gluon density function. The corresponding x and Q^2 values of all these measurements are used in the calcu-

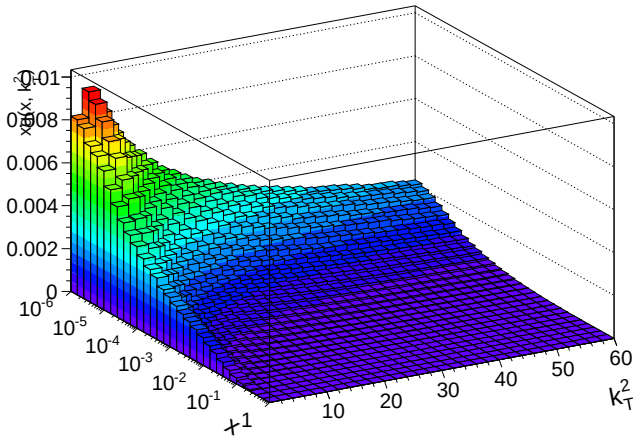

Figure 31: The KMR distribution, calculated from LHAPDF data, at $t = 60$ GeV^2. Normalized to one.

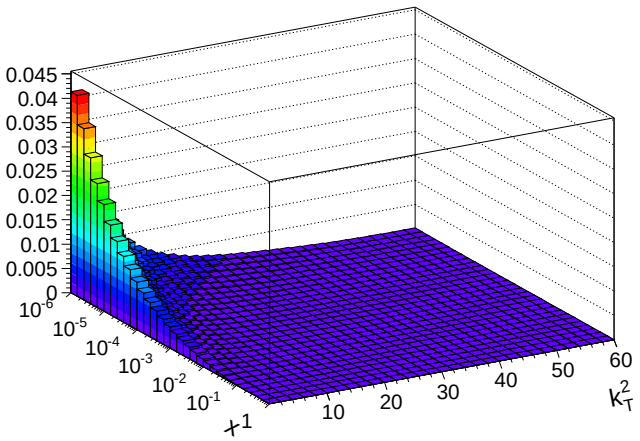

Figure 32: The evolved gluon density function at $t = 60$ GeV^2. Normalized to one.

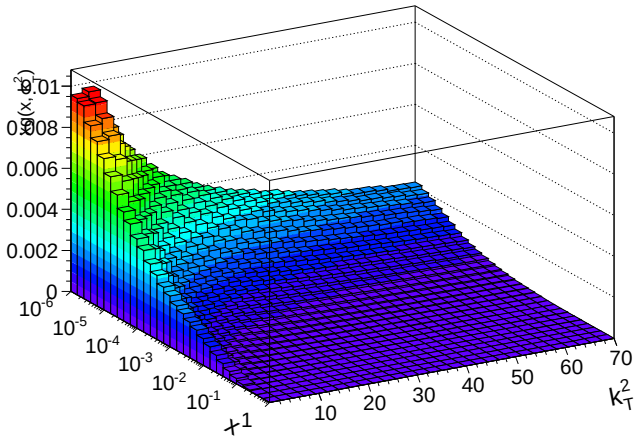

Figure 33: The KMR distribution, calculated from LHAPDF data, at $t = 70$ GeV^2. Normalized to one.

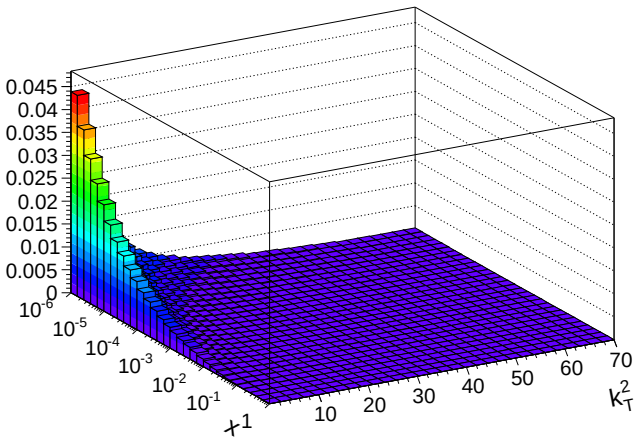

Figure 34: The evolved gluon density function at $t = 70$ GeV^2. Normalized to one.

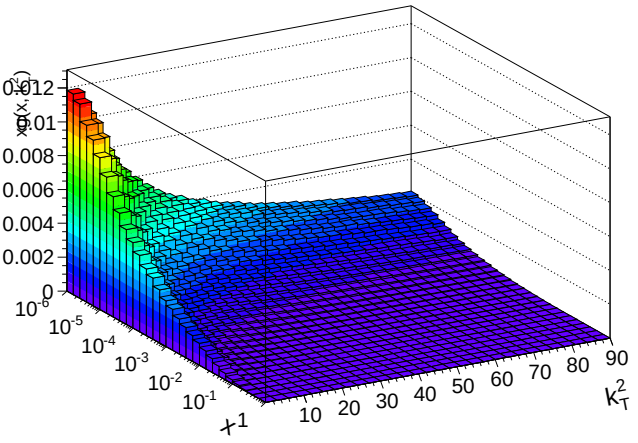

Figure 35: The KMR distribution, calculated from LHAPDF data, at $t = 90$ GeV^2. Normalized to one.

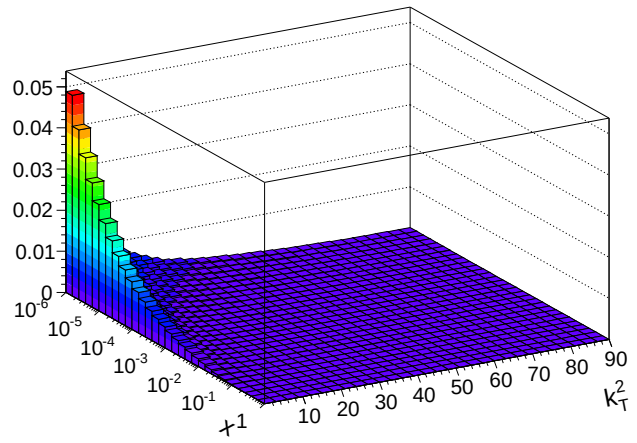

Figure 36: The evolved gluon density function at $t = 90$ GeV^2. Normalized to one.

lation [13] of F_2^g.

3.4.1 k_T independent calculation

$$F_2^g = \int_x^1 dx_g \hat{\sigma}(x_g, Q^2) g(x_g, Q^2) \Theta\left(p_T^2 \geq p_{T,\min}^2\right) \tag{93}$$

where $\hat{\sigma}$ is the cross section for boson-gluon fusion:

$$\hat{\sigma} = \int d\hat{t} \frac{1}{16\pi} \frac{1}{(\hat{s}+Q^2)\hat{s}} |\mathcal{M}|^2 \tag{94}$$

$$|\mathcal{M}|^2 = 32\pi^2 \alpha\alpha_s(Q^2) e_q^2 \frac{1}{2} \left(\frac{\hat{u}}{\hat{t}} + \frac{\hat{t}}{\hat{u}} - \frac{2\hat{s}Q^2}{\hat{u}\hat{t}} \right) \tag{95}$$

with the Mandelstam variables:

$$s = \frac{Q^2}{xy} \tag{96}$$

$$\hat{s} = -Q^2 + yx_g s \tag{97}$$

$$= -Q^2 + yx_g \frac{Q^2}{xy} \tag{98}$$

$$= \frac{x_g - x}{x} Q^2 \tag{99}$$

$$\hat{u} = -Q^2 - \hat{s} - \hat{t}. \tag{100}$$

The integration bounds of $\hat{t}$ are

$$\hat{t}_{\min} = -\varepsilon \tag{101}$$

$$\hat{t}_{\max} = -(Q^2 + \hat{s}) \tag{102}$$

$$= -\left(1 + \frac{x_g - x}{x}\right) Q^2 \tag{103}$$

$$= -\frac{x_g}{x} Q^2. \tag{104}$$

where $\varepsilon = 10^{-4}$ is an arbitrary lower cut-off to prevent a divergency in the calculation of the matrix element (95). The Θ function creates a cut on the p_T^2 of the interaction:

$$p_T^2 = \frac{\hat{s}\hat{t}\hat{u}}{(\hat{s}+Q^2)^2}. \tag{105}$$

This cut on p_T^2 is also arbitrary and has to be determined by comparison with data or another theory.

3.4.2 k_T dependent calculation

This calculation is very similar to the calculation in the section above, with that the difference that the transverse momentum of the incoming gluon is explicitly

[13] F_2 is used to note the `HERA` values of the structure function, F_2^g is used for the calculations based on the gluon density function (hence the g).

mentioned in the calculations. F_2^g is calculated from an unintegrated parton density

$$F_2^g = \int_x^1 dx_g \int_{k_{T,\min}}^{k_{T,\max}} d^2\mathbf{k_T}\hat{\sigma}(x_g, Q^2)g(x_g, k_T^2, Q^2)\Theta\left(p_T^2 \geq p_{T,\min}^2\right) \quad (106)$$

Another difference lies in the value of the Mandelstam variable $\hat{s}$, this is now calculated with k_T.

We know both the incoming photon and gluon to be virtual: they live short enough to be off-shell and thus scale mass-shell equation. In this case the two particles have a non-zero four-momentum squared, which can be interpreted as a non-zero mass. The situation is as follows: a proton P and a photon γ move along the z-axis, towards eachother. In the center-of-mass system they have the same energy and opposed momentum along the z-axis:

$$\begin{aligned} E_P &= E_\gamma & (107)\\ &= |\mathbf{p_P}| & (108)\\ \mathbf{p_P} &= -\mathbf{p}_\gamma. & (109) \end{aligned}$$

The energy of the proton and the photon are the same, and if s is high enough both particles can be considered massless[14] If we follow the mass-shell equation, all energy of the photon and the gluon (in the proton) is stored in the longitudinal momentum $\mathbf{p_z}$. The virtuality of the particles allows them to have mass which will originate from the transverse momentum. The gluon g carries a fraction x_g of the proton's energy and momentum, and has transverse momentum k_T. The photon carries energy E_γ and has transverse momentum Q^2:

$$\begin{aligned} p_g &= (x_g E_P, k_x, k_y, -x_g E_P) & (110)\\ p_\gamma &= \left(E_\gamma, \sqrt{Q^2}\cos\varphi, \sqrt{Q^2}\sin\varphi, E_\gamma\right). & (111) \end{aligned}$$

From this we calculate the total energy of the boson-gluon fusion $\hat{s}$:

$$\begin{aligned} \hat{s} &= (p_g + p_\gamma)^2\\ &= p_g^2 + p_\gamma^2 + 2p_g \cdot p_\gamma\\ &= -k_T^2 - Q^2 + 2x_g E_P E_\gamma - 2\mathbf{p}_g \cdot \mathbf{p}_\gamma\\ &= -k_T^2 - Q^2 + 2x_g E_P E_\gamma - 2p_{g,z}p_{\gamma,z}\\ &= -k_T^2 - Q^2 + 2x_g E_P E_\gamma - 2(-x_g E_P)E_\gamma\\ &= -k_T^2 - Q^2 + 4x_g E_\gamma E_P \end{aligned}$$

where the product of the four-momenta doesn't use the virtual transverse momenta.

The energy of proton and photon are equal and account both for half of the energy available:

$$E = \frac{\sqrt{s}}{2}. \quad (112)$$

[14]The proton has a mass of 1 GeV, which is insignificant compared with the 320 GeV of the collisions.

Including this for the energy in expression (112) yields

$$\hat{s} = -k_T^2 - Q^2 + x_g s. \tag{113}$$

The other two Mandelstam variables can be obtained by adjusting equations (100) and (102). These expressions contain the virtuality of the photon (indicated by a non-zero Q^2) but should also take into account the virtuality of the gluon, which is due to its transverse momentum k_t^2. Transforming the equations is done by replacing Q^2 by $Q^2 + k_T^2$:

$$\hat{u} = -Q^2 - k_T^2 - \hat{s} - \hat{t} \tag{114}$$

$$\hat{t}_{\max} = -\left(Q^2 + k_T^2 + \hat{s}\right) \tag{115}$$

3.4.3 F_2 results

As mentioned above, the structure function is calculated for a certain set of (x, Q^2) values. A first set of calculations was done for all sets ($x < 10^{-2}, Q^2 > 5$ GeV^2), but with different values for $p_{T,\min}^2$ and Λ, and with a different input scale for α_s. These plots are compared and the best scale for α_s is chosen, as well as the best cut on p_T. The plots can be found in appendix D.

The two scales used as input for the coupling are the exchanged four-momentum Q^2 and the transverse momentum p_T^2: if we use Q^2 as the input for the coupling, the resulting F_2 is much less sensitive to a change in Λ. p_T^2 as input for the coupling would result in a value of F_2 that is very sensitive to changes in Λ. Therefore we opt to use Q^2.

It turns out that the ratio F_2^g/F_2 is not a constant in Q^2: we can see that with increasing Q^2 the ratio changes. It is thus not possible to find an ideal value of $p_{T,\min}$ for the entire Q^2 range. For this reason, we choose the sets (x, Q^2) were the ratio between calculation and measurement is very good for a certain cut. These sets are those with $Q^2 = 60$ GeV^2, 70 GeV^2 and 90 GeV^2.

In figures 37, 38 and 39 the ratios F_2^g/F_2 calculated from integrated and unintegrated parton density functions are shown. At each of the three scales both ratios show a decrease with increasing x: this may be a sign that at higher x quarks will play a more prominent role in the calculation of the structure function. In shape there are significant differences between the two ratios at each scale: the transverse momentum of the gluon is important as its presence clearly influences the result. Another reason for this difference could be the Monte Carlo behind the calculations: a higher number of simulated gluons will return a better gluon density function; a higher number of random numbers generated may lead to a better integrated value for F_2. [15]

[15] These calculations would require a more efficient computer than the one that was used for this thesis...

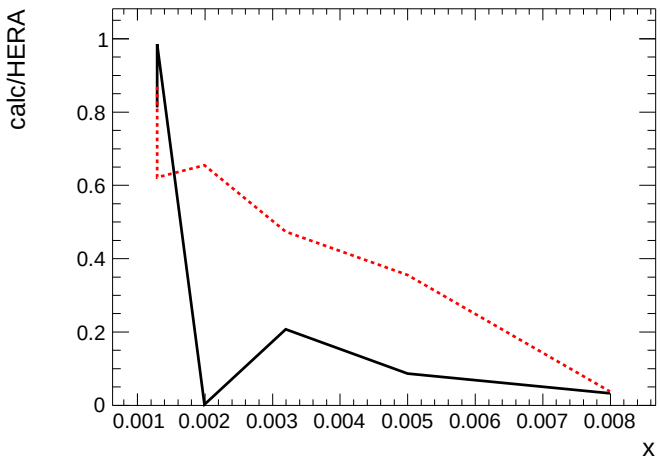

Figure 37: Comparison between ratios F_2^g/F_2 for unintegrated pdf (full black line) and integrated pdf (dashed red line) at scale $Q^2 = 60$ GeV^2.

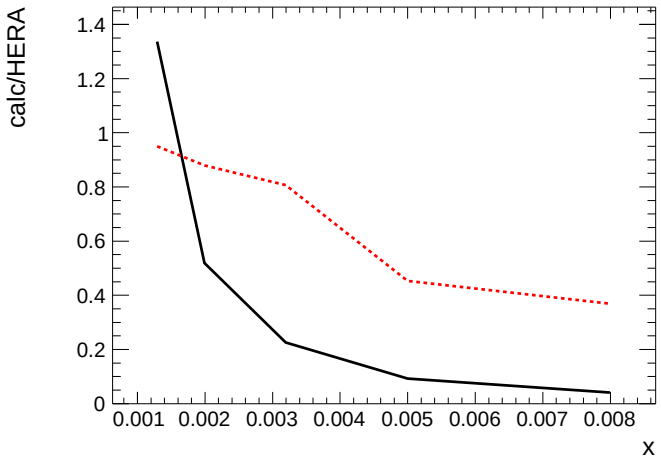

Figure 38: Comparison between ratios F_2^g/F_2 for unintegrated pdf (full black line) and integrated pdf (dashed red line) at scale $Q^2 = 70$ GeV^2.

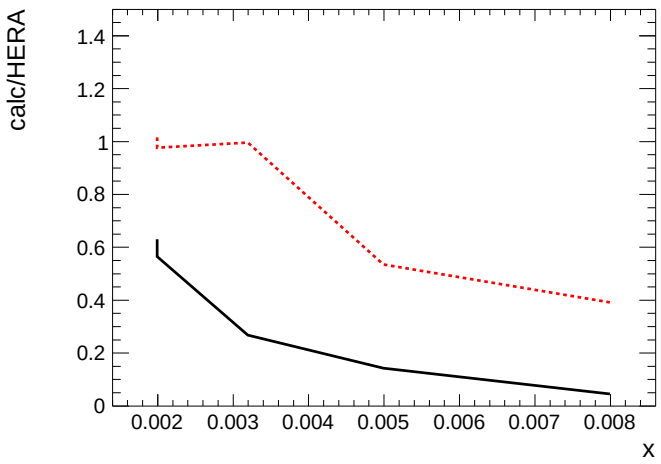

Figure 39: Comparison between ratios F_2^g/F_2 for unintegrated pdf (full black line) and integrated pdf (dashed red line) at scale $Q^2 = 90$ GeV^2.

4 Goals and Conclusions

A first conclusion made in this thesis is that the inclusion of transverse momentum in parton-parton collisions is of great importance. Figure 8 shows that if partons are allowed to build up a large value for transverse momentum k_T, they are able to create high p_T particles even in a two-to-one collision.

A second goal of this thesis was to evolve gluon density functions with a `C++` program. As we can see from the results obtained in section 3.3 the evolution strongly depends on the scale one wishes to use to calculate the coupling strength α_s. The use of transverse momentum p_T as the scale for this coupling will lead to the best evolution results (i.e. the evolved density function will lie the closest to the `LHAPDF` values). However: at high x values the evolved value will be too high and at low x values the evolution will be too low.

Possible reasons for differences between calculations and measurements may be: the lack of quarks in this thesis. We know that the proton is gluon dominated at low x, but at high x quarks are more important. Including the quarks at high x as a gluon emitting source may improve the gluon density function $xg(x)$.

The difference between the updf's from evolution and from `KMR` is, most importantly, the spread in k_T^2 of the `KMR` distribution. The development of transverse momentum in gluon evolution needs to be adjusted, as it should allow for higher transverse momenta.

F_2^g has been calculated from both integrated and unintegrated parton density functions. While the values of F_2^g/F_2 lie in the same order of magnitude for both types of distribution, there are clear difference in shape. This means that one should take k_T^2 in account for the calculation of F_2^g, or that a calculation of the structure function from a updf should be handled differently.

Throughout this thesis several cut-offs were defined. The cut-off on p_T^2 when calculating the ratio of structure functions has a clear influence on the value of the ratio, as can be seen in the appendix. An extra study of the cut-offs used could reveal the sensitivity of the result to these arbitrary values.

Also, one should keep in mind that a series of approximations was used: the splitting function P_{gg} used in the gluon evolution, the analytical expression for the coupling α_s, the absence of quarks... These may have had an effect on the final results.

A Subatomic particles and dynamics

A.1 Four-momentum and the mass shell

Most subatomic particles have a very small mass, if they have one at all. The up and down quark in the proton have masses of just a few MeV, the proton has a mass of nearly 1 GeV. The energies in subatomic physics are nearly always higher than these values, so the particles will be relativistic. This requires the use of four-momentum, which connects mass, energy and momentum. The definition of a four-momentum vector is:

$$\begin{aligned} p &= (p^0, p^1, p^2, p^3) && (116)\\ &= (E, \overrightarrow{p}) && (117) \end{aligned}$$

where E is the energy and $\overrightarrow{p}$ the momentum of a particle. The product of two four-momentum vectors p and q is

$$\begin{aligned} p \cdot q &= (E_p, \overrightarrow{p}) \cdot (E_q, \overrightarrow{q}) && (118)\\ &= E_p E_q - \overrightarrow{p} \cdot \overrightarrow{q} && (119) \end{aligned}$$

Any squared four-momentum p^2 is invariant under Lorentz-transformations, which is the reason we use four-momenta.

The four-momentum connects with the mass via

$$p^2 = m^2 \tag{120}$$

which leads to the mass shell equation:

$$m^2 = E^2 - \overrightarrow{p}^2 \tag{121}$$

A.2 Virtual particles

Any particle whose properties satisfy the relation above is called *on-shell*. These particles are real, and these are the initial and final particles in any Feynman-diagram.

Some particles do not satisfy the mass shell equation: the mass for the particle calculated via this equation will deviate from what we expect. This means that a 91 GeV Z boson could be calculated to have a mass of 100 GeV, or a photon could be massive. Such particles are called *off-shell* and are not real but virtual. The internal particles of a Feynmandiagram are virtual: they exist for a short enough period time to violate the mass shell relation within the bounds of the Heisenberg uncertainty relation

$$\Delta E \Delta t = \hbar. \tag{122}$$

An example of this is an intermediate photon γ between two charged particles. If you would calculate the energy E_γ and momentum $\overrightarrow{p}_\gamma$ of this photon and enter this in the equation of the mass shell, the mass of the photon could be non-zero.

In figure 1 (section 1.3.1) the photon γ has a four-momentum q. Its mass $m_\gamma^2 = q^2$ will not be zero and the quantity $Q^2 = -q^2$ will be a very important one in this thesis.

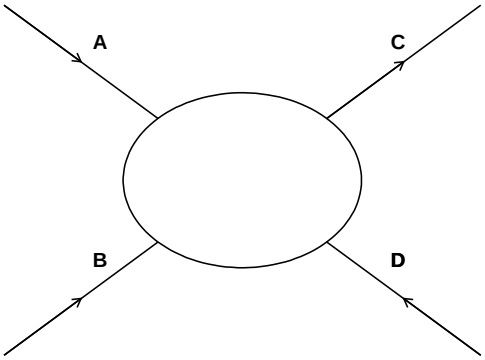

Figure 40: Diagram of a two-to-two particle interaction. The blob in the centre represents all possible interactions between A and B to C and D.

A.3 Mandelstam variables

Due to the relativistic nature of particle physics it will be necesary to take into account Lorentz transformations. Any unaccelerated system has its own interpretation of time, length, energy and momentum. To simplify calculations the Mandelstam variables are used. These are a set of three variables which are Lorentz invariant. If we have an two-to-two interaction as shown in figure 40, then the Mandelstam variables are

$$s = (p_A + p_B)^2 = (p_C + p_D)^2 \quad (123)$$

$$t = (p_A - p_C)^2 = (p_B - p_D)^2 \quad (124)$$

$$u = (p_A - p_D)^2 = (p_B - p_C)^2. \quad (125)$$

If one switches between systems, e.g. from the center-of-mass system to the particle A rest system, the values of s, t and u will not change. $\sqrt{s}$ is the center-of-mass energy: as it is calculated from the sum of four-momenta of the incoming particles, it represents all available energy-momentum of the interaction. If the type of particle doesn't change, i.e. if the reaction is elastic and only a transfer of four-momentum occurs, t can be interpreted as the amount transferred four-momentum squared between the two particles.

The Mandelstam variables are the squares of four-momentum vectors and are numbers. They are linked with eachother via the relation:

$$s + t + u = \sum_{i=a}^{d} m_i^2 \quad (126)$$

One can also work with the quantity $\hat{s}$. If $\sqrt{s}$ is the centre-of-mass energy of an electron-proton collision, then $\sqrt{\hat{s}}$ is the centre-of-mass energy of the actual electron-parton collision. This is shown in figure 1 (section 1.3.1): the electron collides with the proton (s), but the actual interaction is the one between the electron and the quark ($\hat{s}$). As $\hat{s}$ is composed of the energy-momentum of the electron and that of the quark (which is a fraction of that of the proton), $\hat{s}$ is only a fraction of s.

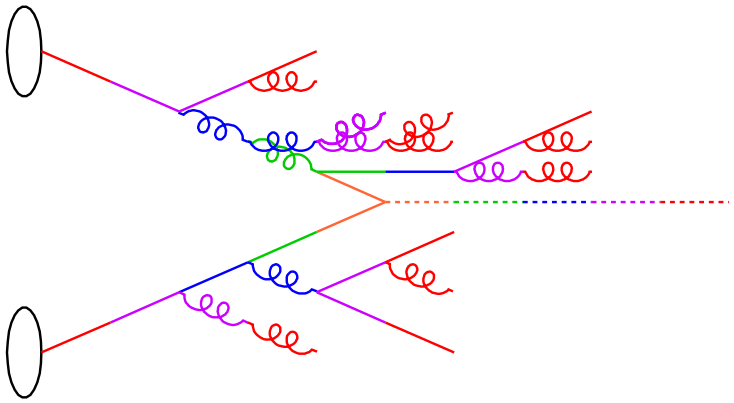

Figure 41: An example of how `Pythia8` works. The diagram is created in different steps. The order of steps is: orange - green - blue - violet - red.

B Extraction of 4D convolution in `Pythia8`

B.1 Names

The particle investigated is called the *current particle*. The two colliding particles are the *initial* quark-antiquark pair. Each particle in `Pythia8` has two *mothers*, particles that lie closer to the proton. These mothers may be two different particles (e.g. the colliding quark and antiquark are the Z' mothers), or it can be just particle (e.g. a quark that didn't radiate any gluons and thus still is a quark). Each particle has two *daughters*, and these can also be two particles (e.g. a gluon split into a quark-antiquark pair) or the same particle (e.g. a non-radiating quark). Two different particles with the same mother are *sisters*, particles that share a part of their ancestry are *cousins*.

B.2 Evolution in `Pythia8`

The different colours used in figure 41 show the time of "creation" of the particle in `Pythia8`'s simulation. The orange lines show the particles that form the core of the diagram: the $q\bar{q} \to Z^0$ collision. `Pythia8` then starts expanding the diagram: the ancestry of the quark-antiquark pair is created as well as the descendants of the Z-boson. For the quarks this means that they become subject to initial state radiation. When researching this ancestry, we often see this quark "change" into a gluon and vice versa.

During the expansion of the diagram kinematic values are added to the particles. The newly created particles are assigned a certain k_T-value. The problem is that particles that are already included in the diagram do not change their k_T-value. For example: when the green particles are added to the diagram, they might have a non-zero k_T-value. The orange particles however do not change: their k_T remains 0. If we wish to calculate the k_T of the orange particles, we will need an algorithm that seeks out all red particles related to them and

make the following sum:

$$k_i(q) = k_i - \sum_n k_i(n) \quad (127)$$

$$k_T(q) = \sqrt{k_x^2(q) + k_y^2(q)} \quad (128)$$

with i the x- or y-component.

Suppose we call the upper orange particle in the diagram the quark, and the lower orange particle the antiquark. Then the transverse momentum of the quark ($k_T(q)$) can be determined by taking the momentum of the parton emitted by the proton (k_T) and subtracting the momenta of all radiated partons ($k_T(n)$). And of course, the vectorial sum $\overrightarrow{k_T}(q) + \overrightarrow{k_T}(\bar{q})$ results in the $\overrightarrow{p_T}$ of the Z^0.

B.3 The algorithm

The outline of the algorithm used is explained in this section.

Each simulation is temporarily saved by `Pythia8` and information about the particles can be accessed, and in later stages processed with the program `Root` [11].

Counting the Z^0-bosons `Pythia8` lets the Z^0-boson decay as soon as the entire diagram (containing parton emission and ISR) is known. The number of incarnations of the Z^0-boson (i.e. the number of colours, if we look at figure 41) in the event is equal to the number of times the diagram has been expanded: we call this variable N.

Finding the emitted partons Having found the value of N, we now proceed to finding the emitted particles. If the number of steps is N then we find the proton after N steps in the ancestry of the colliding quarks. Using the `.mother1()` or `.mother2()` command in `Pythia8`, we get the mother of the colliding particle. Since initial state radiation is allowed, this particle could be a quark of the same flavour as well as a gluon. We set save the mother as the new current particle, and find it's mother. This is repeated until the proton is the mother.

The variable n keeps track of the number of mothers we have found: in the example the green particle would be $n = 1$, the blue particle would be $n = 2$, etc. The mother with $n = N$ is the proton. The particle that has the proton as a mother is thus directly emitted and has the $\overrightarrow{k}$ we need.

Sisters and cousins Everytime the mother of a current particle is found, it is important to check if the current particle has any sisters. The mother of the current particle possibly has two different daughters which can be found via `.daughter1()` and `.daughter2()`. One of them is the current particle, the second one be the sister. If both daughters are not the same particle, we need to investigate the descendants of the sister. If our current mother is $n = s$, then the number of generations descending from our sisterparticle is $N - s$ and the maximum number of possible descendants is 2^{N-s}. All these descendants

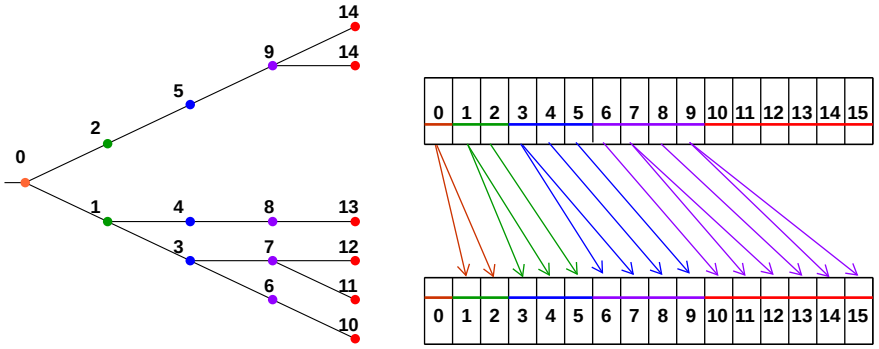

(a) Diagram of sister descendants

(b) Relation of particles in $\mathcal{P}$

Figure 42: Example of how $\mathcal{P}$ is filled. The upper vector shows the parent particles in $\mathcal{P}$ and the arrows show which particles are the daughters of each particle in $\mathcal{P}$. The $\mathcal{G}$ vector is replaced by a colour code: orange - 0, green - 1, blue - 2, purple - 3, red - 4($= N - s$). The particles in (a) are the dots and not the lines. This is not a Feynmandiagram.

are stored in a vector ($\mathcal{P}$), and their generation is stored in a second vector ($\mathcal{G}$) (shown in figure 42). Finding these can be done with the following procedure:

- The first particle stored in $\mathcal{P}$ is the sister, the first slot in $\mathcal{G}$ is "0".
- Then the daughters of the sister are investigated: if they are different, both are added to $\mathcal{G}$, and two slots with their generation ("1") are added to $\mathcal{G}$. If not, the daughter is added only once.
- We move on the next particle in $\mathcal{P}$ and $\mathcal{G}$: what are the daughters, are they identical? Additional slots in both $\mathcal{P}$ and $\mathcal{G}$ appear containing the daughters and their generations.
- This procedure continues until we encounter the value $n - s$ in $\mathcal{G}$: this is the final generation of descendants, these are the particles that contain the right $k_T(n)$ values (red particles in figure 41). All the in $\mathcal{P}$ remaining particles' k_T components are added to the sums $\sum_n k_i$.

This gives us the total $k_T(n)$ contribution by the original sister particle. The procedure above is repeated for each sister in the ancestry.

Figure 42 shows an example of the structure of $\mathcal{P}$. The sister has two different daughters (1 and 2): two new slots are added. Particle 1 has two daughters (two new slots), particle 2 has only one daughter (1 new slot). This repeated until we have found all particles of generation $N-s$. In this case $N-s=4$ and there are four descending generations: green (1), blue (2), purple (3) and red (4). There are six final particles where there might have been as many as $2^{N-s} = 16$. Using $\mathcal{P}$ and $\mathcal{G}$ has a significant effect on the runtime and the memory used.

C Monte Carlo techniques and integration

Some integrals encountered in this thesis can not be solved analytically Using Monte Carlo techniques it is possible to get a solution for these problems. These techniques often use non-uniform random distributions.

C.1 Non-uniform distributions

The random generator used in this thesis is `Ranlux` [7]. This is a uniform random number generator, returning a value R between 0 and 1. It is possible to change both range and shape of this random number distribution. If we wish to generate numbers following a given $g(x)$ distribution between bounds a and b, we need to be able to integrate $g(x)$ analytically. To obtain this non-uniform random number generator, we must solve the following equation:

$$R\int_a^b g(x)dx = \int_a^z g(x)dx \tag{129}$$

and obtain z as a function of the bounds a, b and the uniform random number R.

If we were to use a non-uniform random number generator in a Monte Carlo integral (see section C.2) we would need a weight to compensate for the non-uniform distribution. These weights are calculated as:

$$w(z) = \frac{\int_a^b g(x)dx}{d(z)} \tag{130}$$

where z is the non-uniform random number. Note that this weight can change for different values of z. The exact use of the weight is explained in the next section.

Example A good example of this non-uniform random number generator is the $1/x$ distribution:

$$R\int_a^b \frac{dx}{x} = \int_a^z \frac{1}{x}dx \tag{131}$$

$$R\ln\left(\frac{b}{a}\right) = \ln\left(\frac{z}{a}\right) \tag{132}$$

$$z = a\left(\frac{b}{a}\right)^R. \tag{133}$$

z is now a random number distributed like $1/x$ between a and b. The weight for this distribution would be:

$$w = \frac{\int_a^b \frac{1}{x}dx}{\frac{1}{z}} \tag{134}$$

$$= \ln\left(\frac{b}{a}\right)z. \tag{135}$$

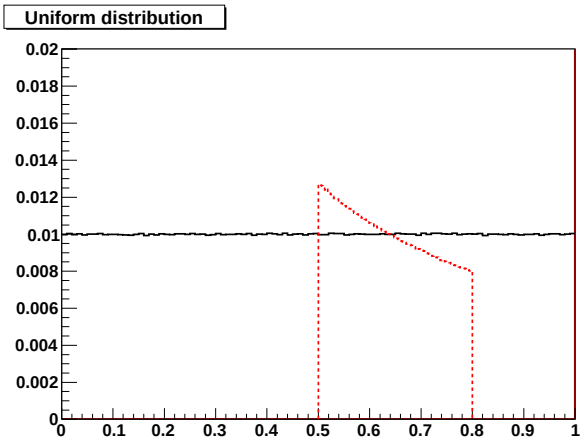

Figure 43: Comparison between uniform random number generator and a custom $\frac{1}{x}$ distribution between 0.5 and 0.8. Both distributions have been normalized to one and were created using the exact same numbers.

Another example is the uniform distribution between bounds b and a:

$$z = R(b-a)+a \tag{136}$$
$$w = b-a. \tag{137}$$

Figure 43 shows two distributions. One is the uniform random number generator between 0 and 1, the other is a $\frac{1}{x}$ between 0.5 and 0.8 using the exact same numbers as the uniform distribution.

C.2 Monte Carlo integration

Any function $f(x)$ can be integrated using the Monte Carlo method, provided that the function "behaves well enough" (has no divergencies) between the bounds of integration. The general expression for Monte Carlo integration is:

$$I_{MC} = \frac{1}{n}\sum_i w_i f(x_i). \tag{138}$$

The variance of this numerical value is:

$$\begin{aligned} V[I_{MC}] &= \sigma_I^2 \\ &= \frac{1}{n}\left[\frac{\sum_i w^2(x_i)f^2(x_i)}{n} - \left(\frac{\sum_i w(x_i)f(x_i)}{n}\right)^2\right]. \end{aligned} \tag{139}$$

We want to able to generate non-uniform random numbers for solving integrals. Suppose a function $f(x)$ has very high values near $x = a$, and very low values near $x = b$. The value of the integral depends more on the function near a, and so we wish to have more random values of x near a. A uniform random generator will treat all parts of $f(x)$ equally, thereby spending as much time on the unimportant as the important parts. We would be obligated to

choose between fast runtime but very inaccurate values for the integral, or more precise results after a long runtime. The use of a custom random number generator increases accuracy while reducing runtime by paying more attention to the important parts of the integral.

D Structure function F_2 results

In this section the different ratios between calculation and measurement of the proton structure function F_2^g are shown for comparison. F_2^g is calculated using equation (93). The values for $g(x_g, Q^2)$ are taken from `LHAPDF`: there is no explicit gluon evolution executed. In each plot three different p_T cuts are shown: $p^2_{T,\min} = 0.1$ GeV^2, 0.5 GeV^2 and 1 GeV^2. The expression for p_T^2 is (105).

The values $F_2(x, Q^2)$ are taken from the `HERA` data [14]. Note that each datapoint from `HERA` is also connected with a inelasticity y and collision energy s. These four variables depend on each other via

$$sxy = Q^2.$$

Since the absolute values of y and s do not matter when we calculate the structure function from an integrated parton density function, we fix $y = 1$ and calculate s from the three independent variables. This means that not all collisions of the `HERA` data are executed at the same center-of-mass energy.

On the left hand side, F_2 is calculated with Q^2 as the scale in α_s. On the right hand side, we use p_T^2 as a scale for the coupling.

The results are divided into three sections, each using a different value for Λ. Λ is not a constant [6], so we need to know how sensitive the calculations are to any changes in Λ.

D.1 $\Lambda = 200$ MeV

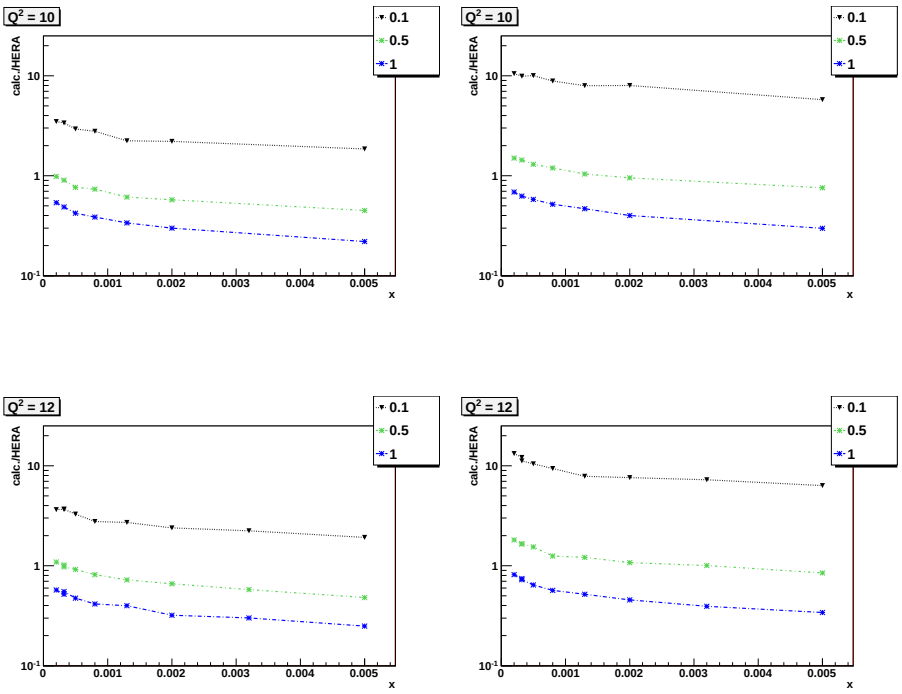

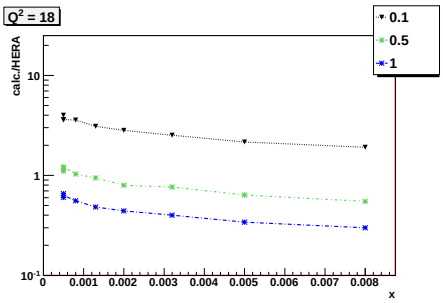
Q^2 = 18
0.1
0.5
1
calc./HERA
10
1
10^{-1}
0
0.001
0.002
0.003
0.004
0.005
0.006
0.007
0.008
x

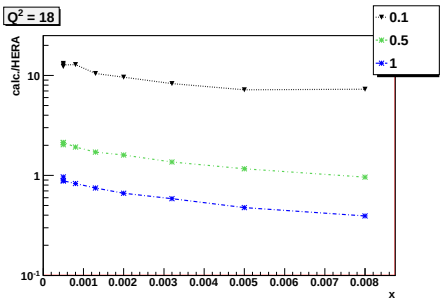
Q^2 = 18
0.1
0.5
1
calc./HERA
10
1
10^{-1}
0
0.001
0.002
0.003
0.004
0.005
0.006
0.007
0.008
x

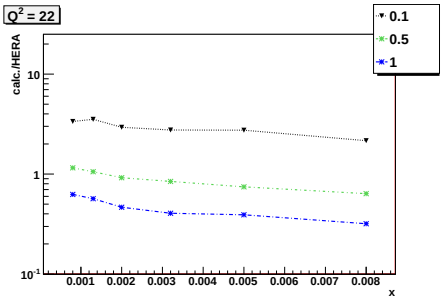
Q^2 = 22
0.1
0.5
1
calc./HERA
10
1
10^{-1}
0.001
0.002
0.003
0.004
0.005
0.006
0.007
0.008
x

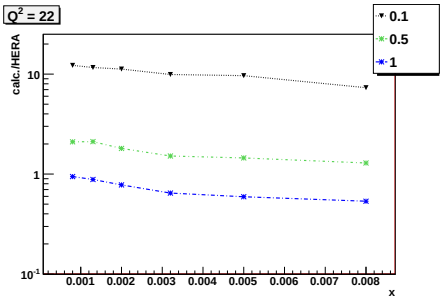
Q^2 = 22
0.1
0.5
1
calc./HERA
10
1
10^{-1}
0.001
0.002
0.003
0.004
0.005
0.006
0.007
0.008
x

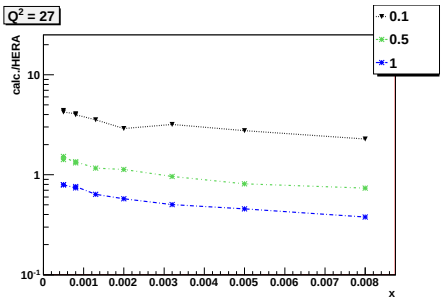
Q^2 = 27
0.1
0.5
1
calc./HERA
10
1
10^{-1}
0
0.001
0.002
0.003
0.004
0.005
0.006
0.007
0.008
x

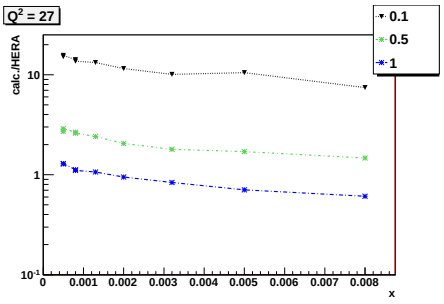
Q^2 = 27
0.1
0.5
1
calc./HERA
10
1
10^{-1}
0
0.001
0.002
0.003
0.004
0.005
0.006
0.007
0.008
x

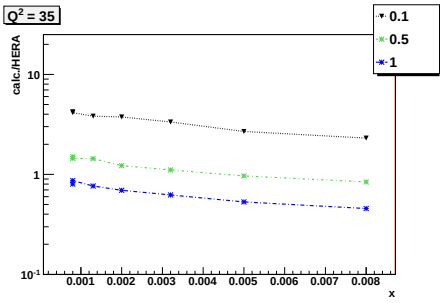
Q^2 = 35
0.1
0.5
1
calc./HERA
10
1
10^{-1}
0.001
0.002
0.003
0.004
0.005
0.006
0.007
0.008
x

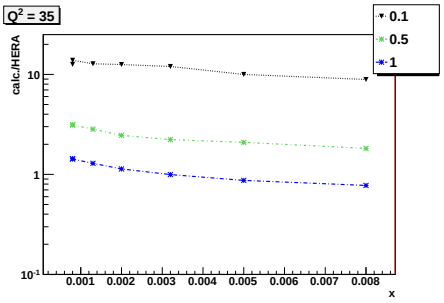
Q^2 = 35
0.1
0.5
1
calc./HERA
10
1
10^{-1}
0.001
0.002
0.003
0.004
0.005
0.006
0.007
0.008
x

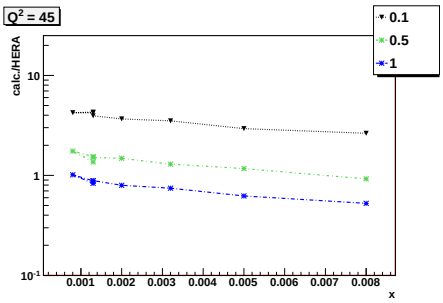
Q^2 = 45
0.1
0.5
1
calc./HERA
10
1
10^{-1}
0.001 0.002 0.003 0.004 0.005 0.006 0.007 0.008
x

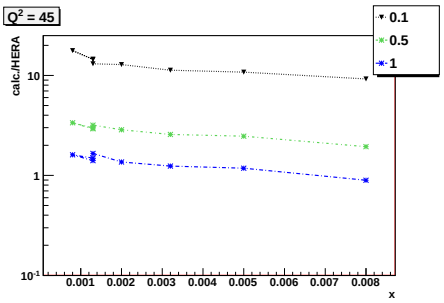
Q^2 = 45
0.1
0.5
1
calc./HERA
10
1
10^{-1}
0.001 0.002 0.003 0.004 0.005 0.006 0.007 0.008
x

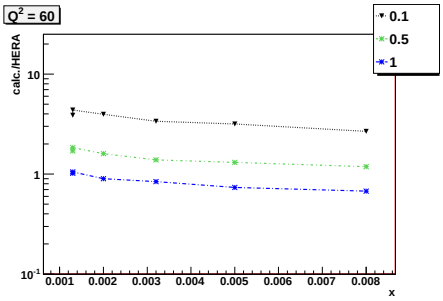
Q^2 = 60
0.1
0.5
1
calc./HERA
10
1
10^{-1}
0.001 0.002 0.003 0.004 0.005 0.006 0.007 0.008
x

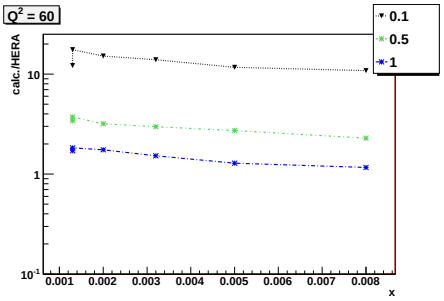
Q^2 = 60
0.1
0.5
1
calc./HERA
10
1
10^{-1}
0.001 0.002 0.003 0.004 0.005 0.006 0.007 0.008
x

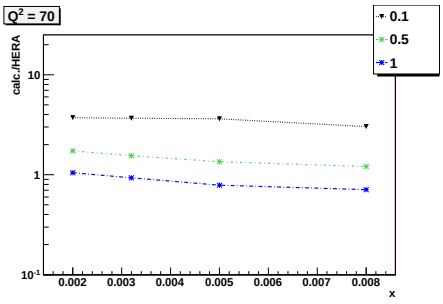
Q^2 = 70
0.1
0.5
1
calc./HERA
10
1
10^{-1}
0.002 0.003 0.004 0.005 0.006 0.007 0.008
x

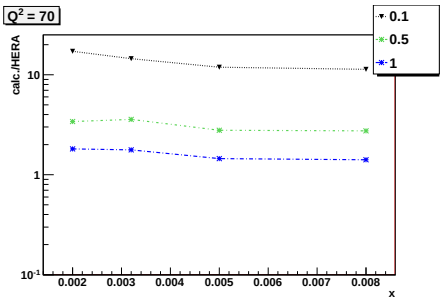
Q^2 = 70
0.1
0.5
1
calc./HERA
10
1
10^{-1}
0.002 0.003 0.004 0.005 0.006 0.007 0.008
x

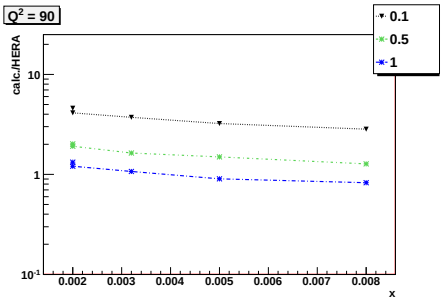
Q^2 = 90
0.1
0.5
1
calc./HERA
10
1
10^{-1}
0.002 0.003 0.004 0.005 0.006 0.007 0.008
x

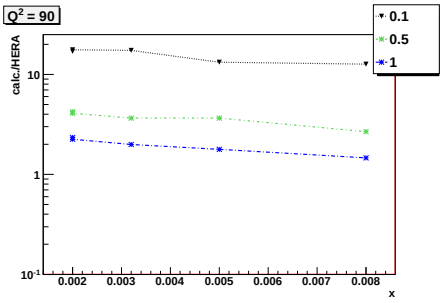
Q^2 = 90
0.1
0.5
1
calc./HERA
10
1
10^{-1}
0.002 0.003 0.004 0.005 0.006 0.007 0.008
x

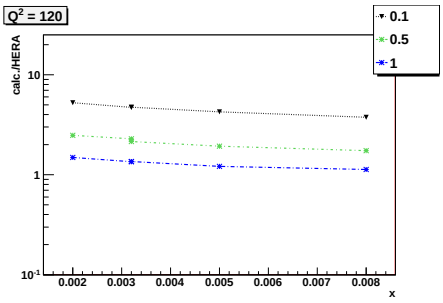
Q^2 = 120
0.1
0.5
1
calc./HERA
10
1
10^{-1}
0.002
0.003
0.004
0.005
0.006
0.007
0.008
x

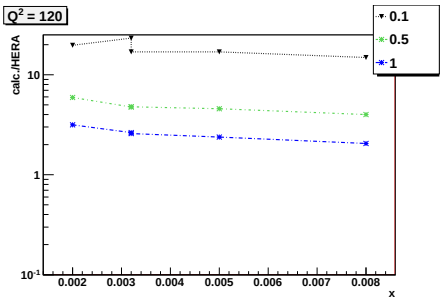
Q^2 = 120
0.1
0.5
1
calc./HERA
10
1
10^{-1}
0.002
0.003
0.004
0.005
0.006
0.007
0.008
x

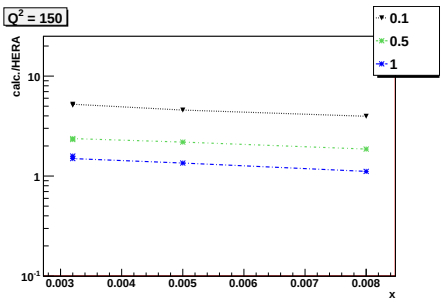
Q^2 = 150
0.1
0.5
1
calc./HERA
10
1
10^{-1}
0.003
0.004
0.005
0.006
0.007
0.008
x

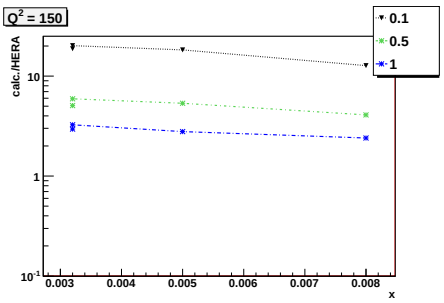
Q^2 = 150
0.1
0.5
1
calc./HERA
10
1
10^{-1}
0.003
0.004
0.005
0.006
0.007
0.008
x

D.2 $\Lambda = 250$ MeV

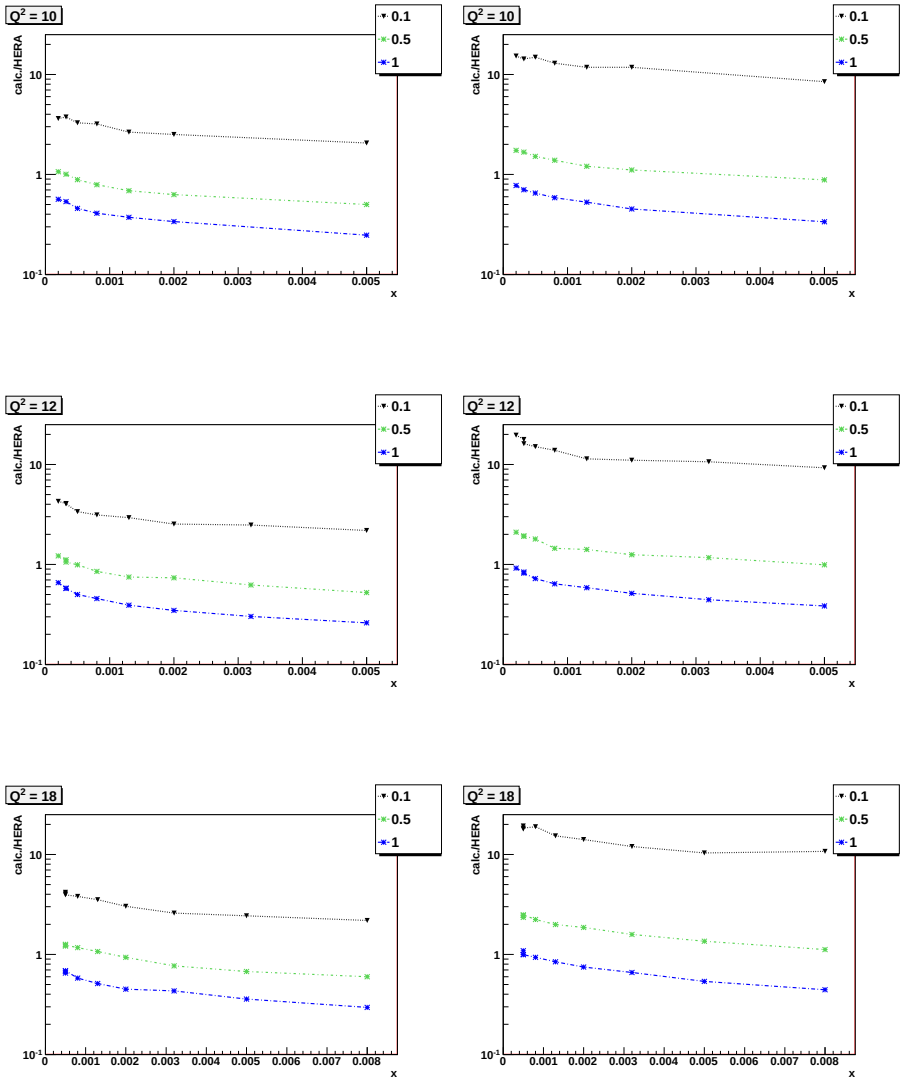

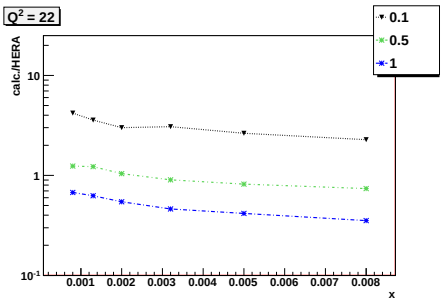
Q^2 = 22
0.1
0.5
1
calc./HERA
10
1
10^{-1}
0.001 0.002 0.003 0.004 0.005 0.006 0.007 0.008
x

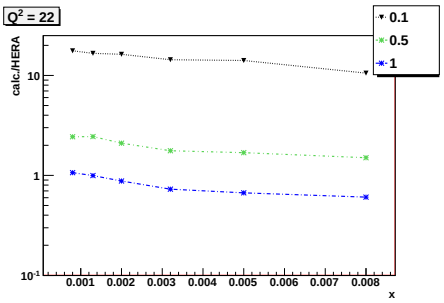
Q^2 = 22
0.1
0.5
1
calc./HERA
10
1
10^{-1}
0.001 0.002 0.003 0.004 0.005 0.006 0.007 0.008
x

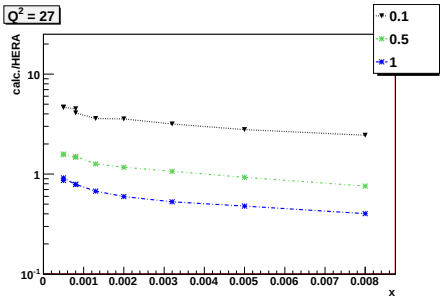
Q^2 = 27
0.1
0.5
1
calc./HERA
10
1
10^{-1}
0 0.001 0.002 0.003 0.004 0.005 0.006 0.007 0.008
x

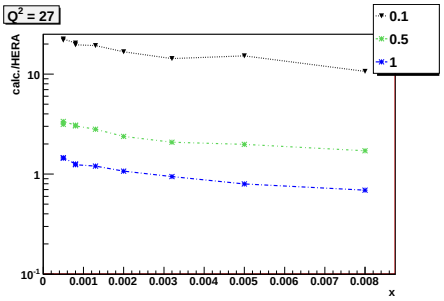
Q^2 = 27
0.1
0.5
1
calc./HERA
10
1
10^{-1}
0 0.001 0.002 0.003 0.004 0.005 0.006 0.007 0.008
x

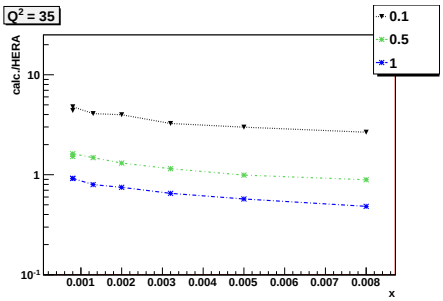
Q^2 = 35
0.1
0.5
1
calc./HERA
10
1
10^{-1}
0.001 0.002 0.003 0.004 0.005 0.006 0.007 0.008
x

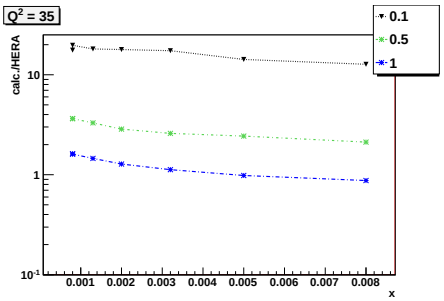
Q^2 = 35
0.1
0.5
1
calc./HERA
10
1
10^{-1}
0.001 0.002 0.003 0.004 0.005 0.006 0.007 0.008
x

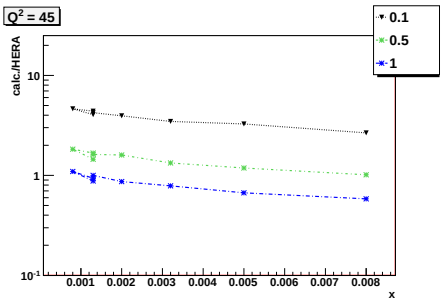
Q^2 = 45
0.1
0.5
1
calc./HERA
10
1
10^{-1}
0.001 0.002 0.003 0.004 0.005 0.006 0.007 0.008
x

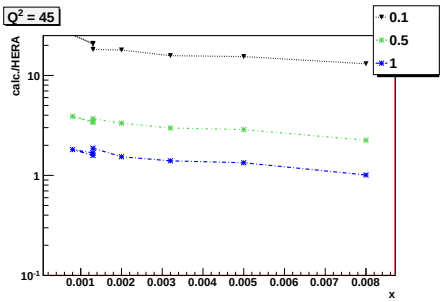
Q^2 = 45
0.1
0.5
1
calc./HERA
10
1
10^{-1}
0.001 0.002 0.003 0.004 0.005 0.006 0.007 0.008
x

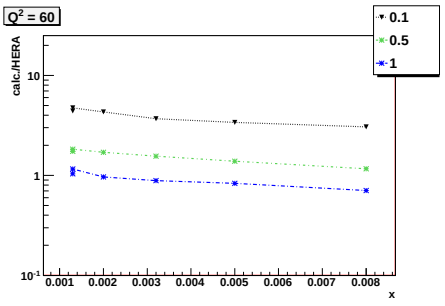
Q^2 = 60
0.1
0.5
1
calc./HERA
10
1
10^{-1}
0.001 0.002 0.003 0.004 0.005 0.006 0.007 0.008
x

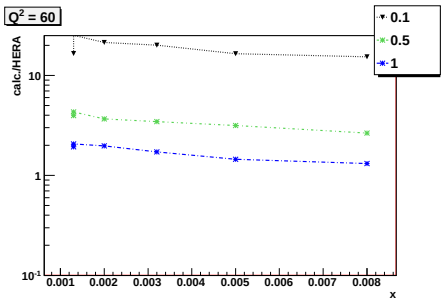
Q^2 = 60
0.1
0.5
1
calc./HERA
10
1
10^{-1}
0.001 0.002 0.003 0.004 0.005 0.006 0.007 0.008
x

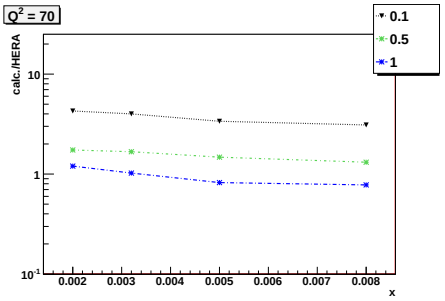
Q^2 = 70
0.1
0.5
1
calc./HERA
10
1
10^{-1}
0.002 0.003 0.004 0.005 0.006 0.007 0.008
x

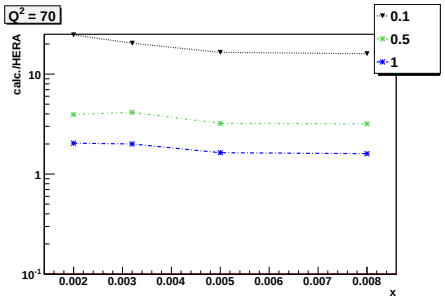
Q^2 = 70
0.1
0.5
1
calc./HERA
10
1
10^{-1}
0.002 0.003 0.004 0.005 0.006 0.007 0.008
x

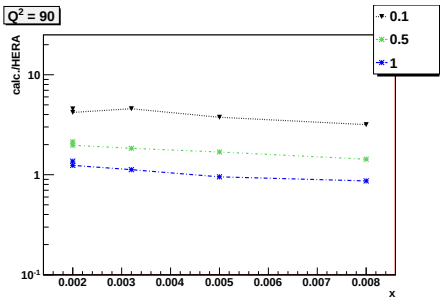
Q^2 = 90
0.1
0.5
1
calc./HERA
10
1
10^{-1}
0.002 0.003 0.004 0.005 0.006 0.007 0.008
x

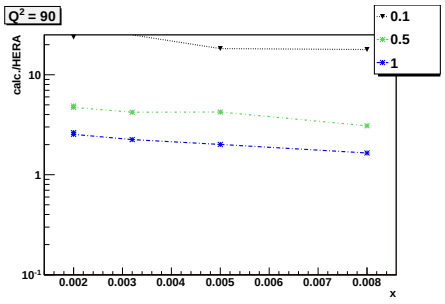
Q^2 = 90
0.1
0.5
1
calc./HERA
10
1
10^{-1}
0.002 0.003 0.004 0.005 0.006 0.007 0.008
x

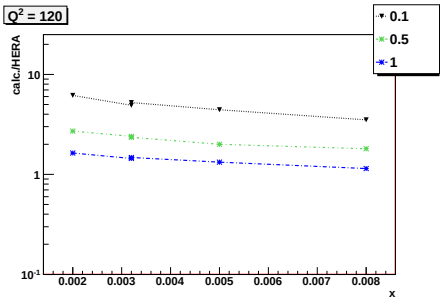
Q^2 = 120
0.1
0.5
1
calc./HERA
10
1
10^{-1}
0.002 0.003 0.004 0.005 0.006 0.007 0.008
x

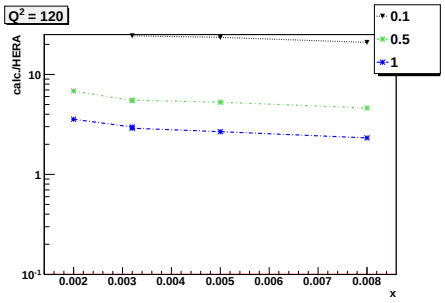
Q^2 = 120
0.1
0.5
1
calc./HERA
10
1
10^{-1}
0.002 0.003 0.004 0.005 0.006 0.007 0.008
x

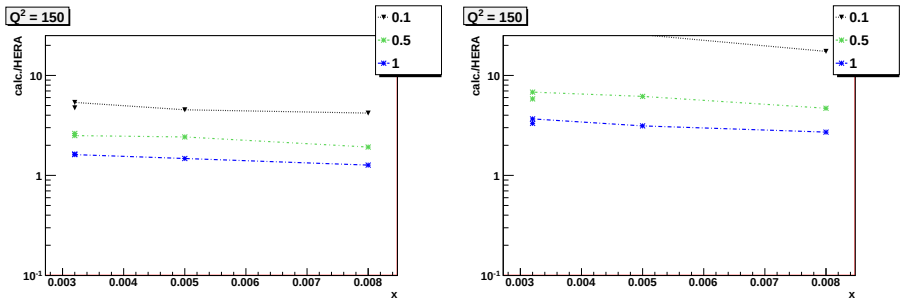
Q^2 = 150
0.1
0.5
1
calc./HERA
10
1
10^{-1}
0.003
0.004
0.005
0.006
0.007
0.008
x
Q^2 = 150
0.1
0.5
1
calc./HERA
10
1
10^{-1}
0.003
0.004
0.005
0.006
0.007
0.008
x

D.3 $\Lambda = 300$ MeV

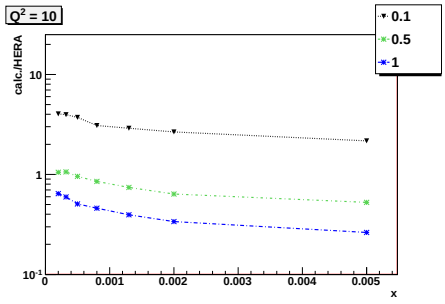

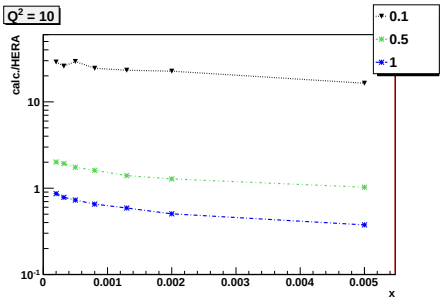

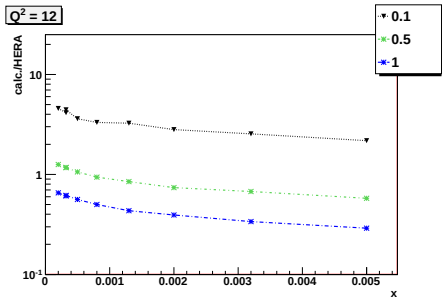

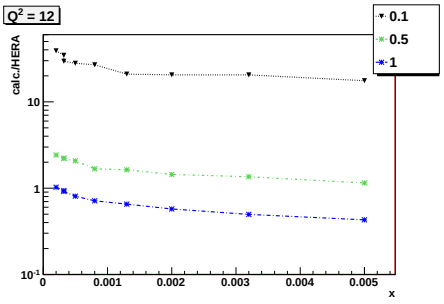

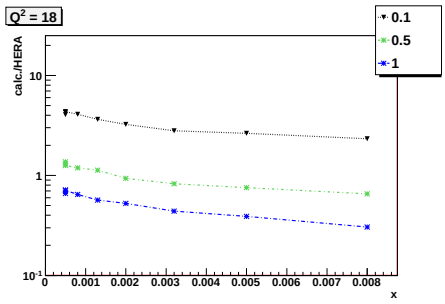

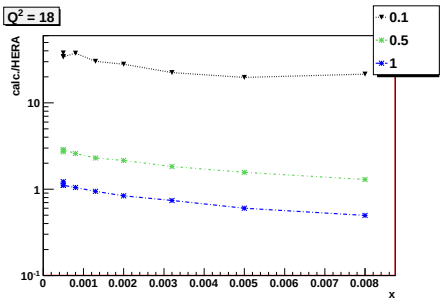

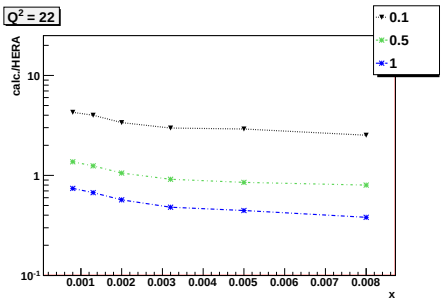
Q^2 = 22
0.1
0.5
1
calc./HERA
10
1
10^{-1}
0.001 0.002 0.003 0.004 0.005 0.006 0.007 0.008
x

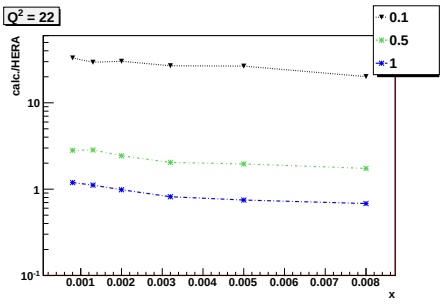
Q^2 = 22
0.1
0.5
1
calc./HERA
10
1
10^{-1}
0.001 0.002 0.003 0.004 0.005 0.006 0.007 0.008
x

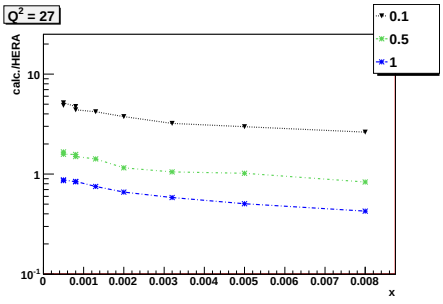
Q^2 = 27
0.1
0.5
1
calc./HERA
10
1
10^{-1}
0 0.001 0.002 0.003 0.004 0.005 0.006 0.007 0.008
x

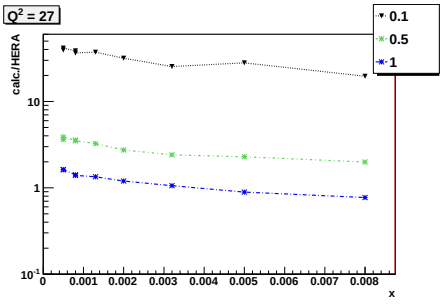
Q^2 = 27
0.1
0.5
1
calc./HERA
10
1
10^{-1}
0 0.001 0.002 0.003 0.004 0.005 0.006 0.007 0.008
x

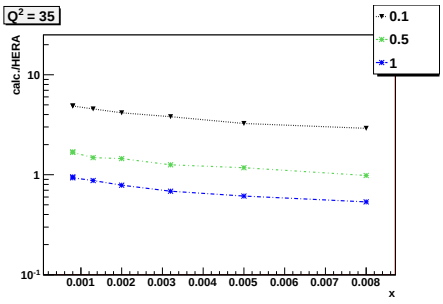
Q^2 = 35
0.1
0.5
1
calc./HERA
10
1
10^{-1}
0.001 0.002 0.003 0.004 0.005 0.006 0.007 0.008
x

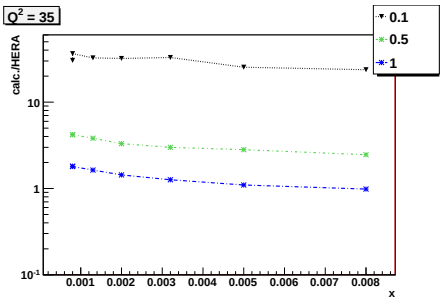
Q^2 = 35
0.1
0.5
1
calc./HERA
10
1
10^{-1}
0.001 0.002 0.003 0.004 0.005 0.006 0.007 0.008
x

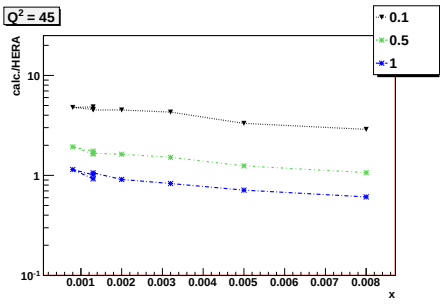
Q^2 = 45
0.1
0.5
1
calc./HERA
10
1
10^{-1}
0.001 0.002 0.003 0.004 0.005 0.006 0.007 0.008
x

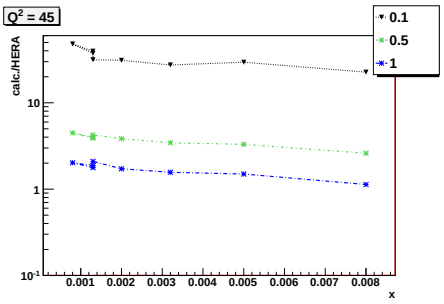
Q^2 = 45
0.1
0.5
1
calc./HERA
10
1
10^{-1}
0.001 0.002 0.003 0.004 0.005 0.006 0.007 0.008
x

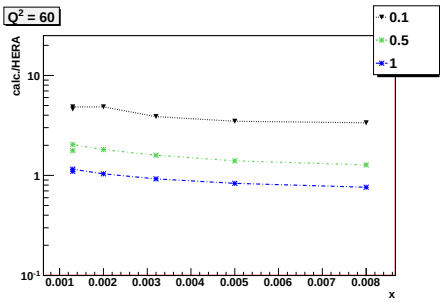
Q^2 = 60
0.1
0.5
1
calc./HERA
10
1
10^{-1}
0.001 0.002 0.003 0.004 0.005 0.006 0.007 0.008
x

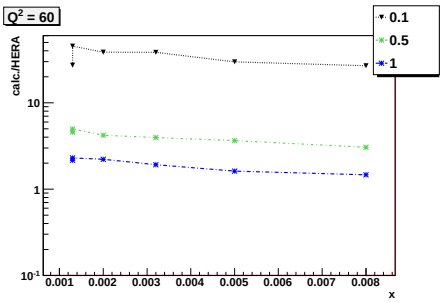
Q^2 = 60
0.1
0.5
1
calc./HERA
10
1
10^{-1}
0.001 0.002 0.003 0.004 0.005 0.006 0.007 0.008
x

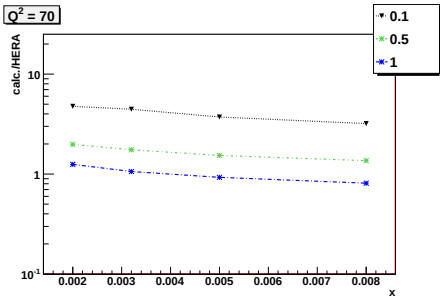
Q^2 = 70
0.1
0.5
1
calc./HERA
10
1
10^{-1}
0.002 0.003 0.004 0.005 0.006 0.007 0.008
x

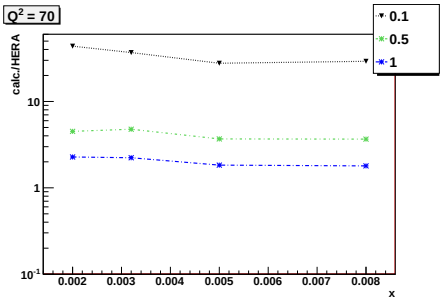
Q^2 = 70
0.1
0.5
1
calc./HERA
10
1
10^{-1}
0.002 0.003 0.004 0.005 0.006 0.007 0.008
x

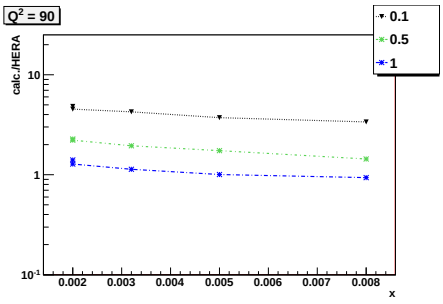
Q^2 = 90
0.1
0.5
1
calc./HERA
10
1
10^{-1}
0.002 0.003 0.004 0.005 0.006 0.007 0.008
x

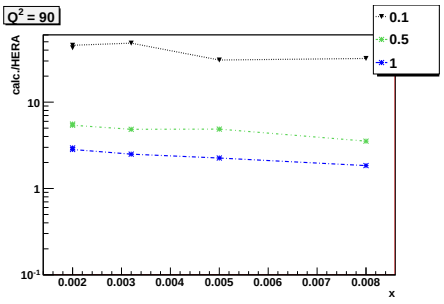
Q^2 = 90
0.1
0.5
1
calc./HERA
10
1
10^{-1}
0.002 0.003 0.004 0.005 0.006 0.007 0.008
x

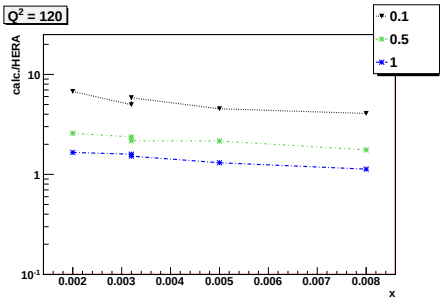
Q^2 = 120
0.1
0.5
1
calc./HERA
10
1
10^{-1}
0.002 0.003 0.004 0.005 0.006 0.007 0.008
x

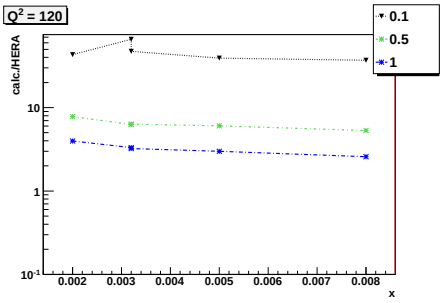
Q^2 = 120
0.1
0.5
1
calc./HERA
10
1
10^{-1}
0.002 0.003 0.004 0.005 0.006 0.007 0.008
x

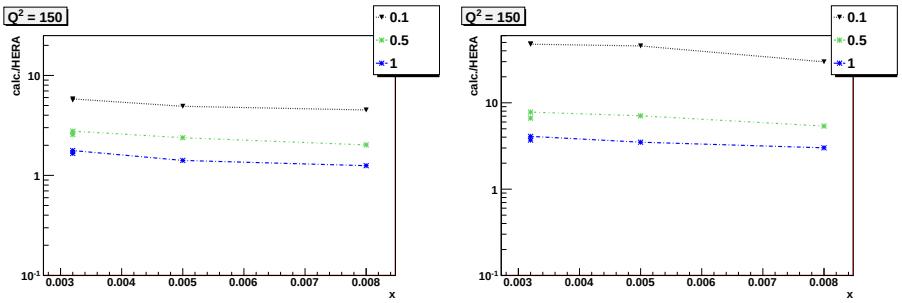
Q^2 = 150
0.1
0.5
1
calc./HERA
10
1
10^{-1}
0.003
0.004
0.005
0.006
0.007
0.008
x
Q^2 = 150
0.1
0.5
1
calc./HERA
10
1
10^{-1}
0.003
0.004
0.005
0.006
0.007
0.008
x

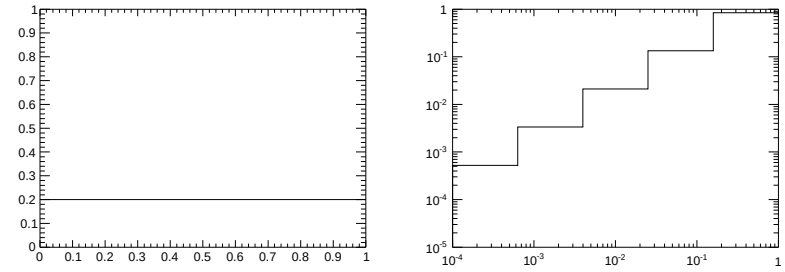

Figure 44: The left plot shows linear binning, the right plot shows logarithmic binning.

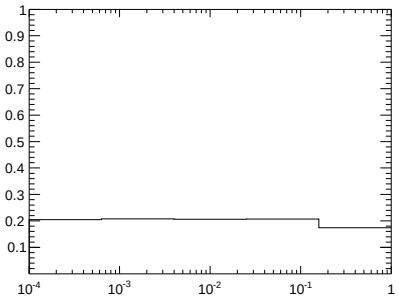

Figure 45: The logarithmic binning plot where each of the bins has been divided by its binwidth.

E Logarithmic bins

Some plots in this thesis use a logarithmic x-axis (or y-axis, in 3D histograms). This results in different binwidths: a bin between $x = 10^{-6}$ and $x = 10^{-5}$ will be ten times smaller than a bin between $x = 10^{-5}$ and $x = 10^{-4}$. Different binwidths may lead to confusing results or incorrect interpretations: a uniform distribution will not be flat. Figure shows two different versions of the same plot: N uniform random numbers have been generated and entered in both histograms.

The shape of the histogram with logarithmic bins does not lead to the conclusion that the distribution was uniform. By dividing each bin by its width the histogram becomes clear.

References

[1] A.D. Martin, "Proton structure, Partons, QCD, DGLAP and beyond", arXiv:0802.0161v1 [hep-ph]

[2] Particle Data Group (PDG), "2011 Summary Tables", http://pdg.lbl.gov/2011/tables/contents_tables.html.

[3] P. Van Mechelen, "Subatomaire fysica", Universiteit Antwerpen, Academic year 2008-2009.

[4] H. Jung, "QCD and MC Lectures".

[5] R.K. Ellis, W.J. Stirling, B.R. Webber, "QCD and Collider Physics", Cambridge, Cambridge University Press, ed. 2003.

[6] W. J. Marciano, "Flavor Thresholds and Λ in the Modified Minimal-Substraction Scheme", Physical Review D, Vol. 29, N. 3, 1 February 1984.

[7] M. Lüscher, "Ranlux - A portable high-quality random number generator for lattice field theory simulations", Computer Physics Communications 79 (1994) 100, http://luscher.web.cern.ch/luscher/ranlux/index.html

[8] T. Sjöstrand, "Pythia", http://home.thep.lu.se/ torbjorn/Pythia.html

[9] M.A. Kimber, A.D. Martin, M.G. Ryskin, "Unintegrated parton distributions", arXiv:hep-ph/0101348v1

[10] M. Whalley, A. Buckley, "LHAPDF::HepForge", http://projects.hepforge.org/lhapdf/

[11] The ROOT Team, "ROOT — A Data Analysis Framework", http://root.cern.ch/drupal/

[12] K. Nakamura et al. (Particle Data Group), J. Phys. G 37, 075021 (2010). Cut-off date for this update was January 15, 2010.

[13] H1 Collaboration, "Measurement of the Inclusive ep Scattering Cross Section at Low Q^2 and x at HERA", DESY 08-171, August 2009.

[14] HERA Collaboration, "HERA Combined Results", https://www.desy.de/h1zeus/combined_results/index.php